TADCs derived from TRAMP mice showed higher expression of several chemokine/cytokines and, interestingly, immunosuppressive genes including *Ido1*, *Arg1*, *Cd274* (*PD-L1*) and *Foxo3*.

Tumor-associated DCs derived from TRAMP mice are immunosuppressive, tolerogenic and induce suppressive activity in tumor-specific T cells; therefore, the authors investigated which molecule is responsible. Blockade of PD-1 and TGF-β, as well as inhibition of IDO1 and ARG, inhibited the tolerogenic ability, but the effects were partial. Then, the authors focused on one transcription factor Foxo3, which is overexpressed in TADCs compared with DCs from wild-type mice, as Foxo3 deficiency resulted in hypersensitivity in a previous study [3]. Genetic knockdown of *Foxo3* pDCs reduced the expression of immunosuppressive genes including *Ido1* and *Arg1* and secretion of TGF-β, and prevented T-cell tolerance both in a TRAMP prostate cancer model and B16 melanoma model. Interestingly, transfer of T helper cells into TRAMP mice reduced the expression of *Ido1*, *Arg1* and *Foxo3* in TADCs, as well as inhibiting their suppressive functions, but the effect was partial.

Finally, the authors evaluated human TADCs to validate whether same phenomenon can be observed in also human specimens. In human TADCs, tolerogenic genes including *IDO1*, *PD-L1*, *FAS-LG* and *FOXO3* were overexpressed, and silencing of the *FOXO3* gene abrogated tolerogenicity and T-cell-induced immune suppression.

Discussion & significance

The authors described an aspect of molecular mechanisms involved in immune tolerance of antitumor immunity. They succeeded to demonstrate this in both mouse model and human specimens. This is the first report describing FOXO3 involvement in immune tolerance by TADCs; however, the molecular mechanisms of upstream signaling of FOXO3 are still elusive. FOXO3 has been identified a tumor suppressor inducing p27 following G1 arrest [7]. FOXO3 has been described to protect quiescent cells from oxidative stress inducing manganese superoxide dismutase (*MnSOD*) gene [8]. Generally, cancer cells grow very fast and the environment within cancer tissues is usually hypoxic; therefore, hypoxic stress might induce the expression of *FOXO3* in TADCs.

The molecular mechanisms of downstream signaling of FOXO3 are also still elusive. FOXO3 is a transcription factor; therefore it may induce tolerogenic genes including *IDO1*, *ARG1*, *PD-L1* and *TGF*-β directly or indirectly through inducing intermediate molecules. Inhibition or blockade of immune suppressing genes including *IDO1*, *ARG1*, *PD-L1* and *TGF*-β cancelled the torelogenicity of TADCs partially, but not completely. These results suggest that there should be more downstream factors involved in tolerance, and further analysis is expected.

Future perspective

FOXO3 gene silencing might be a good strategy to inhibit immune tolerance; however, nonspecific siRNA transfer into tumors might be unbeneficial for cancer patients, because FOXO3 works also as a tumor suppressor and is expressed in ubiquitous cells. Therefore, establishment of the gene transfer modality or vectors for specific targeting tumor-associated pDCs should be essential for the achievement of effective anti-immunotolerance therapy that targets FOXO3.

Financial & competing interests disclosure

This work was supported by a Grant-in-Aid for Scientific Research from the Ministry of Education, Culture, Sports, Science and Technology in Japan (to N Sato) and Program for Developing the Supporting System for Upgrading Education and Research from the Ministry of Education, Culture, Sports, Science and Technology of Japan (to N Sato). The authors have no other relevant affiliations or financial involvement with any organization or entity with a financial interest in or financial conflict with the subject matter or materials discussed in the manuscript apart from those disclosed.

No writing assistance was utilized in the production of this manuscript.

Executive summary

- *FOXO3* is expressed in plasmacytoid tumor-associated dendritic cells infiltrated in human prostate cancer tissues and tissues from TRAMP mouse models of prostate cancer.
- FOXO3 induced tolerogenic genes including *IDO1*, *ARG* and *TGF*-β, and induced antitumor immunity tolerance.
- Gene silencing of *FOXO3* inhibited the tolerogenic activity of tumor-associated dendritic cells.

Bibliography

1 Rosenberg SA, Yang JC, Restifo NP. Cancer immunotherapy: moving beyond current vaccines. *Nat. Med.* 10(9), 909–915 (2004).

2 Yu H, Pardoll D, Jove R. STATs in cancer inflammation and immunity: a leading role for STAT3. *Nat. Rev. Cancer* 9(11) 798–809 (2009).

3 Dejean AS, Beisner DR, Ch'en IL *et al.* Transcription factor Foxo3 controls the magnitude of T cell immune responses by modulating the function of dendritic cells. *Nat. Immunol.* 10(5), 504–513 (2009).

4 Watkins SK, Zhu Z, Riboldi E *et al.* FOXO3 programs tumor-associated DCs to become tolerogenic in human and murine prostate cancer. *J. Clin. Invest.* 121(4), 1361–1372 (2011).

5 Anderson MJ, Shafer-Weaver K, Greenberg NM, Hurwitz AA. Tolerization of tumor-specific T cells despite efficient initial priming in a primary murine model of prostate cancer. *J. Immunol.* 178(3), 1268–1276 (2007).

6 Shafer-Weaver KA, Anderson MJ, Stagliano K, Malyguine A, Greenberg NM, Hurwitz AA. Cutting edge: tumor-specific CD8$^+$ T cells infiltrating prostatic tumors are induced to become suppressor cells. *J. Immunol.* 183(8), 4848–4852 (2009).

7 Medema RH, Kops GJ, Bos JL, Burgering BM. AFX-like Forkhead transcription factors mediate cell-cycle regulation by Ras and PKB through p27kip1. *Nature* 404(6779), 782–787 (2000).

8 Kops GJ, Dansen TB, Polderman PE *et al.* Forkhead transcription factor FOXO3a protects quiescent cells from oxidative stress. *Nature* 419(6904), 316–321 (2002).

J Cancer Res Clin Oncol (2011) 137:789–794
DOI 10.1007/s00432-010-0940-6

ORIGINAL PAPER

Autoantibody against hypoxia-inducible factor prolyl hydroxylase-3 is a potential serological marker for renal cell carcinoma

Toshiaki Tanaka · Hiroshi Kitamura · Toshihiko Torigoe · Yoshihiko Hirohashi · Eiji Sato · Naoya Masumori · Noriyuki Sato · Taiji Tsukamoto

Received: 24 April 2010 / Accepted: 18 July 2010 / Published online: 31 July 2010

Abstract
Purpose To verify the efficacy of a serum autoantibody against hypoxia-inducible factor prolyl hydroxylase-3 (PHD3) as a serological marker for RCC.
Methods Serum samples and surgically resected tumor tissue specimens were obtained from 22 patients with primary RCC, 15 of whom underwent radical nephrectomy and 7 partial nephrectomy. Preoperative serum samples were obtained just before tumor resection. Postoperative serum samples were obtained from 17 patients at least 1 month after tumor removal. Serum samples were also obtained from 26 healthy volunteers. Titers of the anti-PHD3 antibody (Ab) were determined by enzyme-linked immunosorbent assay.
Results Serum anti-PHD3 Ab titers were significantly higher in patients with RCC than in healthy volunteers (0.610 ± 0.023 vs. 0.591 ± 0.031, $P = 0.0001$). Using a cutoff point of 0.599, sensitivity, specificity, and positivity for prediction of RCC were 86.4, 57.7, and 63.3%, respectively. In all 17 patients, titers of serum anti-PHD3 were decreased after the surgical resection compared with those before operation (0.622 ± 0.023 vs. 0.580 ± 0.024, $P = 0.0003$).
Conclusions The present study suggests that the anti-PHD3 Ab may be a novel serological marker for RCC and the titer may reflect the tumor burden in each individual.

Keywords Renal cell carcinoma · Tumor marker · Autoantibody · PHD3 protein

T. Tanaka (✉) · H. Kitamura · E. Sato · N. Masumori · T. Tsukamoto
Department of Urology,
Sapporo Medical University School of Medicine,
S-1, W16, Chuo-ku, Sapporo, Hokkaido 060-8543, Japan
e-mail: zappa@pop12.odn.ne.jp

T. Torigoe · Y. Hirohashi · N. Sato
1st Department of Pathology,
Sapporo Medical University School of Medicine,
Sapporo, Hokkaido, Japan

Introduction

In the United States, it was estimated that in 2009 there were 57,760 new cases of kidney cancer and 12,980 cancer-related deaths (Jemal et al. 2009). Renal cell carcinoma (RCC) accounts for around 95% of kidney cancers and is the most lethal of the genitourinary tract malignancies. The development and diffusion of diagnostic imaging technology have contributed to discovery of an increased number of small tumors and decreased death from RCC. However, the cost-effectiveness of screening using ultrasonography or computed tomography is still controversial due to the relatively low incidence of RCC (Campbell et al. 2007). Therefore, discovery of diagnostic biomarkers of RCC in serum or urine samples is much awaited. Biomarkers may also be helpful for differential diagnosis of radiographically equivalent renal tumors such as complicated cysts and angiomyolipoma lacking a fat component. In addition, they may be useful to distinguish metastatic or recurrent disease from nonspecific nodular lesions in follow-up examinations after surgical treatment.

For various other cancers, several autoantibodies against cancer-specific antigens have been investigated as serological tumor markers (Barua et al. 2007; Larsson et al. 2006; Nilsson et al. 2001; Shimada et al. 2000, 2002; Suzuki et al. 2004; Takeda et al. 2001a, b; Tan and Zhang 2008; Zhong et al. 2008). We previously reported that an autoantibody

against a cancer-specific antigen could be detected in sera of patients with RCC (Kitamura et al. 2007). In addition, we found that hypoxia-inducible factor prolyl hydroxylase-3 (PHD3) was frequently overexpressed in cancer tissue of renal cell carcinomas (RCCs) with high specificity to cancer tissue and demonstrated its usefulness as a novel tumor antigen in immunotherapy for RCC (Sato et al. 2008).

PHD3 is one member of the PHD family, which is involved in the degradation of hypoxia-inducible factor (HIF) proteins in cooperation with von-Hippel Lindau protein under normoxic conditions. HIF, a transcriptional factor, induces the expression of more than 60 target genes such as vascular endothelial growth factor (VEGF) and erythropoietin, which play roles in tumor progression and contribute to tumor aggressiveness (Maynard and Ohh 2007) under hypoxic conditions.

In the current study, we verified the availability of an anti-PHD3 antibody (Ab) as a serological marker for RCC.

Materials and methods

After informed consent was obtained from the 22 patients with RCC, serum samples and surgically resected tumor tissue specimens were collected from the 15 patients who underwent radical nephrectomy and 7 who underwent partial nephrectomy. The study was performed after approval of the institutional review board. The median age at operation for the 11 men and 11 women was 63.5 years (range 35–82). Histological examination was done with hematoxylin and eosin-stained slides, and clinical stage was assigned according to the 2002 TNM classification of malignant tumors (Sobin and Wittekind 2002). Preoperative blood samples were collected just before tumor resection, and postoperative ones were obtained from 17 patients 1 month after surgery. We also collected blood samples from 26 healthy volunteers (age range 22–66 years) after receipt of informed consent. After centrifugation, sera were divided into aliquots and stored at −80°C. Tumor tissue specimens were immersed in RNAlater solution (Ambion, Austin, TX) immediately after removal and incubated at 4°C overnight, then stored at −80°C.

Reverse transcription-polymerase chain reaction (RT-PCR) was performed by the following procedure. Total ribonucleic acid (RNA) was isolated from tumor tissue using an RNeasy Mini Kit (Qiagen, Valencia, CA). A complementary deoxyribonucleic acid (cDNA) mixture was synthesized from 2 μg of total RNA by reverse transcription using SuperScript III and oligo (dT) primer (Invitrogen, Carlsbad, CA) according to the manufacturer's protocol. PCR amplification was done in 50 μL of PCR mixture containing 1 μL of cDNA mixture, 1 μL of KOD Plus DNA polymerase (Toyobo, Osaka, Japan), and 15 pmol primers. The PCR mixture was initially incubated at 94°C for 2 min followed by 35 cycles of denaturation as 94°C for 15 s, annealing at 64°C for 30 s, and extension at 72°C for 30 s. The primer pair 5′-CATCCCTGTCTTGT GTGTGG-3′ (forward) and 5′-CCAACAGCCCTGGATT AAGA-3′ (reverse) was employed for specific detection of PHD3. The expected size of the PCR product was 420 bp. As an internal control, glyceraldehyde-3-phosphate dehydrogenase expression was detected using forward primer 5′-ACCACAGTCCATGCCATCAC-3′ and reverse primer 5′-TCCACCACCCTGTTGCTGTA-3′ with an expected PCR product of 452 bp. The PCR products were visualized with ethidium bromide staining under ultraviolet light following electrophoresis on 1.0% agarose gel.

Recombinant PHD3 protein was produced and purified as described previously (Sato et al. 2008; Yagihashi et al. 2003). For production of the protein, the RT-PCR product amplified from the initial 300 bp of the PHD3 gene was used. The calculated molecular weight was 11.0 kDa. Enzyme-linked immunosorbent assay (ELISA) was performed for detection of the anti-PHD3 Ab in each serum as previously described (Yagihashi et al. 2003). The absorbance was measured at 450 nm. Data were obtained in triplicate for each sample. Western blot analysis of serum anti-PHD3 Ab was also performed to confirm the specificity of immunoreactivity to PHD3 protein. Recombinant PHD3 protein and bovine serum albumin were boiled in Laemmli buffer and resolved by sodium dodecylsulfate polyacrylamide gel electrophoresis. The proteins were transferred to polyvinylidene difluoride membranes (Immobilon-P, Millipore, Bedford, MA), which were then incubated with serum samples diluted 1:10 followed by a 1:2,000 dilution of goat anti-human immunoglobulin G F(ab')2 conjugated with horseradish peroxidase (DakoCytomation, Glostrup, Denmark). The immunocomplex was visualized by enhanced chemiluminescence according to the manufacturer's specifications (Amersham Biosciences, Piscataway, NJ).

We compared the values for the anti-PHD3 Ab between two groups by using the Mann-Whiney U test and the Wilcoxon signed-rank test. $P < 0.05$ was considered to indicate statistical significance. Receiver operating characteristics (ROC) analysis was used to determine the area under the curve (AUC), sensitivity, and specificity for prediction of RCC.

Results

RT-PCR analysis revealed that PHD3 was overexpressed in 21 (95.4%) of the 22 RCC specimens. The results of RT-PCR analysis and ELISA detecting the serum anti-PHD3 Ab, and the relationship to clinicopathologic characteristics are summarized in Table 1. All patients with stage

Table 1 Clinicopathological characteristics, PHD3 mRNA expression and serum anti-PHD3 antibody titers in patients with renal cell carcinoma

No.	Histological type	Clinical stage	PHD3 mRNA expression	Anti-PHD3 antibody	
				Before	After
1	Clear	T1bN0M0	Negative	0.625	N.A.
2	Clear	T1bN0M0	Positive	0.617	0.555
3	Clear	T1aN0M0	Positive	0.598	0.566
4	Clear	T1aN0M0	Positive	0.607	0.589
5	Clear	T2N0M0	Positive	0.611	0.571
6	Clear	T1aN0M0	Positive	0.607	0.602
7	Clear	T1aN0M0	Positive	0.620	0.584
8	Clear	T1bN0M0	Positive	0.638	0.598
9	Spindle	T2N1M1	Positive	0.633	0.574
10	Clear	T1aN0M0	Positive	0.648	0.600
11	Clear	T1aN0M0	Positive	0.660	0.598
12	Clear	T2N0M0	Positive	0.678	0.651
13	Clear	T1aN0M0	Positive	0.609	N.A.
14	Clear	T1aN0M0	Positive	0.600	0.576
15	ACDK	T1aN0M0	Positive	0.595	N.A.
16	Clear	T1aN0M0	Positive	0.599	0.551
17	Chromophobe	T1aN0M0	Positive	0.607	0.565
18	Clear	T1bN0M0	Positive	0.603	0.564
19	Clear	T1aN0M0	Positive	0.579	N.A.
20	Clear	T2N0M0	Positive	0.623	0.560
21	TFE3 fusion	T1aN0M0	Positive	0.630	0.564
22	Clear	T1aN0M0	Positive	0.621	N.A.

Clear clear cell carcinoma, *Spindle* spindle cell carcinoma, *ACDK*, RCC associated with acquired cystic disease of the kidney in a chronic hemodialysis patient, *Chromophobe* chromophobe cell carcinoma, TFE3 fusion, *RCC* associated with Xp11.2/TFE3 gene fusion, *Before* before surgery, *After* after surgery, *N.A.* not available

I–II disease underwent complete surgical resection. On the other hand, one stage IV patient (Case 9) had multiple metastases to the lung and abdominal lymph nodes at the time of radical nephrectomy; therefore, she did not become free from disease after the operation. There was no significant correlation between disease stage and the anti-PHD3 Ab titer.

The median absorbance values of ELISA detecting the anti-PHD3 Ab in sera from patients with RCC and healthy volunteers were 0.614 (0.579–0.678) and 0.597 (0.473–0.621), respectively (Fig. 1a). There was a significant difference between them ($P = 0.0007$). The cutoff value for positivity in the anti-PHD3 ELISA was determined to be 0.599, according to ROC-AUC analysis (Fig. 1b). On the basis of this criterion, the sensitivity, specificity, and positive predictive value for RCC were 86.4, 57.7, and 63.3%, respectively.

Western blot analysis for the serum anti-PHD3 Ab in a patient with RCC demonstrated immunoreactivity to recombinant PHD3 protein. On the other hand, there was no immunoreactivity in serum from a healthy volunteer with a low titer in the anti-PHD3 ELISA (Fig. 1c).

The titers of the anti-PHD3 Ab before and after surgical resection were compared individually in 17 patients with RCC (Fig. 2). The anti-PHD3 Ab titer was decreased after the operation in all of them, with statistical significance ($P = 0.0003$), and 14 (83.4%) showed conversion to a seronegative condition with a cutoff value of 0.599.

Discussion

PHDs are involved in the degradation of hypoxia-inducible factor (HIF) proteins in cooperation with von-Hippel Lindau (VHL) protein. A member of the family, PHD3 is frequently overexpressed in RCCs, but barely in normal tissues (Sato et al. 2008). The putative expression mechanism is stable accumulation of HIF protein due to VHL gene inactivation. In this study, however, PHD3 overexpression at the messenger RNA (mRNA) level was equally observed even in RCC tissues unrelated to mutation or epigenetic modification of the VHL gene such as in chromophobe cell carcinoma and spindle cell carcinoma. Tissue hypoxia may also lead to PHD3 expression, because the catalytic activity of PHD3 is oxygen-dependent, and hypoxia may induce accumulation of unhydroxylated and undegradated HIF proteins (Appelhoff et al. 2004; Cioffi et al. 2003; Hirsilä et al. 2003). One patient (Case 1) had a high titer of the anti-PHD3 Ab despite the lack of expression of PHD3 mRNA in the RCC tissue. RT-PCR for

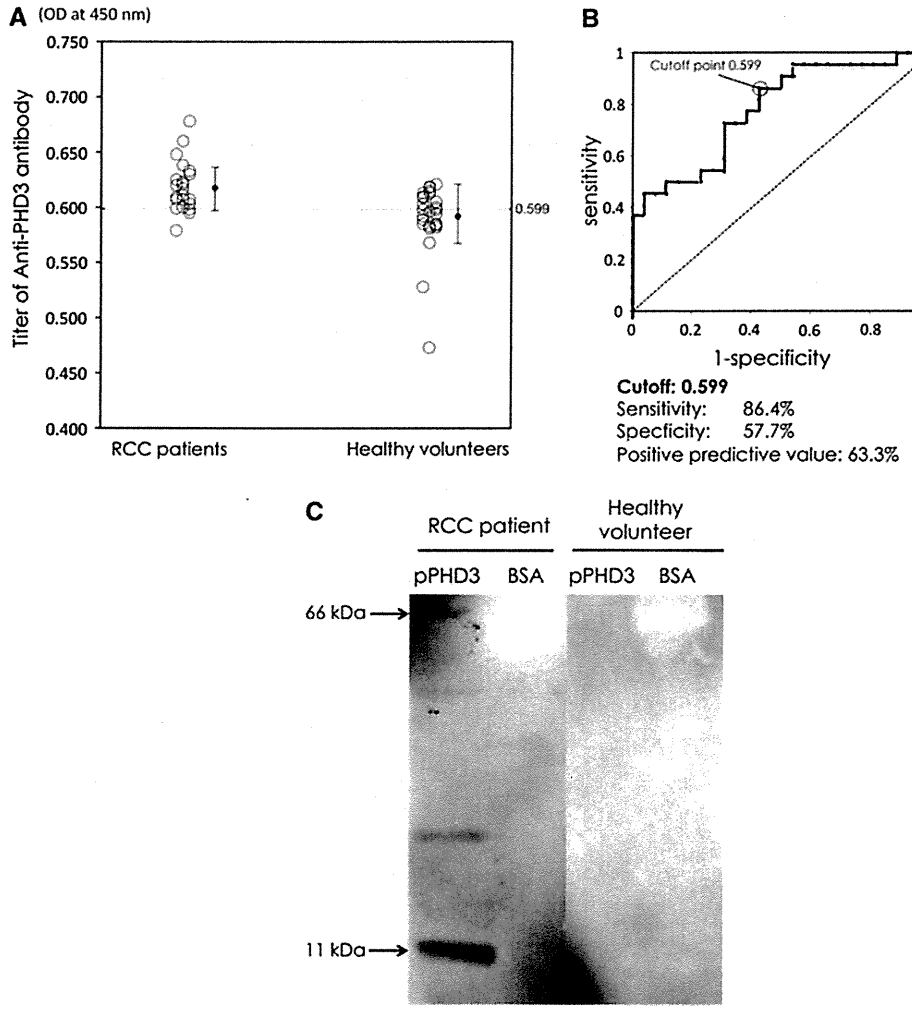

Fig. 1 **a** Serum anti-PHD3 Abs of patients with RCC and healthy volunteers. *Error bars* indicate mean ± standard deviation. **b** Receiver operating characteristic plot for cutoff point of serum anti-PHD3 Ab titer to predict RCC. **c** Western blot analysis for immunoreactivity of serum to PHD3 recombinant protein. *Lanes 1* and *2*, serum from a patient with RCC. *Lanes 3* and *4*, serum from a healthy volunteer. The *bars* of 66 kDa and 11 kDa indicate molecular sizes of bovine serum albumin and recombinant protein of PHD3, respectively. pPHD3, PHD3 recombinant protein; BSA, bovine serum albumin

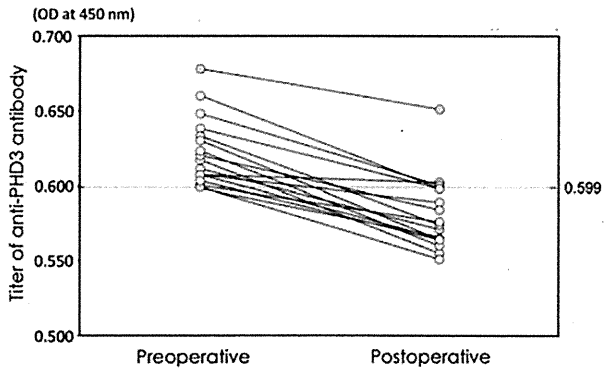

Fig. 2 Changes of serum anti-PHD3 Ab titers after surgical resection

detection of PHD3 was performed with only a small part of the RCC tissue, so it is speculated that we may have failed to obtain a PHD3-positive area.

Various autoantibodies against cancer-specific antigens have been investigated to verify their potential as serological tumor markers. Autoantibodies against p53, IMP, p62, Koc, c-myc, cyclin-B1, and survivin were reported to be useful for detection of malignant tumors of various origins such as those of the esophagus, colorectum, bladder, prostate, stomach, liver, pancreas, lung, breast, and ovary (Barua et al. 2007; Larsson et al. 2006; Nilsson et al. 2001; Shimada et al. 2000, 2002; Suzuki et al. 2004; Takeda et al. 2001a, b; Tan and Zhang 2008: Zhong et al. 2008). In RCC, we previously reported that livin, a member of the inhibitor of apoptosis protein family, was recognized as a tumor-specific antigen in patients and anti-livin autoantibodies were detected in their sera (Kitamura et al. 2007). In addition, we found that PHD3 was recognized as a cancer-specific antigen and might be a target in immunotherapy for RCC (Sato et al. 2008). To the best of our knowledge, this is the first report demonstrating the efficacy of an autoantibody against a cancer-specific antigen as a serological marker for RCC.

The current study has limitations. Many individuals were included in the marginal zone, and 42.3% of the

healthy volunteers were positive for serum anti-PHD3 Abs, with a cutoff point of 0.599. The assay possibly detected nonspecific immune reactions. That is probably also the reason why there was a discrepancy between the result of the ELISA and the seronegativity shown by Western blotting in a healthy volunteer. Furthermore, PHD3 may be expressed in normal tissues other than those screened in our previous study (Sato et al. 2008). Although the specificity was low, our results showed the feasibility of an autoantibody against an anti-tumor antigen as a serological marker for RCC. The anti-PHD3 Ab can potentially facilitate the efficient selection of candidates for further radiographical examinations and may contribute to improvement of the cost-effectiveness of screening examinations for RCC. Further studies, in which patients are followed for long periods and the serum anti-PHD3 Ab level is regularly tested, are needed to determine its clinical usefulness.

All patients with RCC displayed decreases in the titer of the autoantibody after tumor resection, as shown in studies of an anti-p53 Ab in esophageal squamous cell carcinoma (Shimada et al. 2000, 2002) and colorectal adenocarcinoma (Takeda et al. 2001a, b). This finding suggests that the titer of the anti-PHD3 autoantibody may reflect the volume of the disease. In addition, Shimada et al. (2000, 2002) reported that persistent seropositivity for an anti-p53 Ab was associated with future disease recurrence in patients with esophageal cancer, which might indicate small residual cancer after surgery. In this study, some patients with clinically organ-confined disease still had high titers of the anti-PHD3 Ab after surgical resection, though the titers decreased. Although changes in the titer may be associated with the amount of cancer in each individual, we could not conclude that postoperative titers of serum anti PHD3 Ab can predict microscopic residual cancer or future disease recurrence. To confirm that, monitoring of the PHD3 Ab titer in follow-up and verification of the association between the disease recurrence and increase in the titer is necessary.

Conclusions

We demonstrated that the anti-PHD3 Ab titer was significantly higher in the sera of patients with RCC than in healthy volunteers. In addition, the anti-PHD3 Ab titers decreased in all patients with RCC after surgical resection. Although there are some limitations, these findings suggest that the anti-PHD3 Ab is a potential serological marker for RCC.

Acknowledgments The authors thank Ryoji Furuya for his kind assistance with data collection.

Conflict of interest We declare that we have no conflict of interest.

References

Appelhoff RJ, Tian YM, Raval RR, Turley H, Harris AL, Pugh CW, Ratcliffe PJ, Gleadle JM (2004) Differential function of the prolyl hydroxylases PHD1, PHD2, and PHD3 in the regulation of hypoxia-inducible factor. J Biol Chem 279:38458–38465

Barua A, Bradaric MJ, Kebede T, Espionosa S, Edassery SL, Bitterman P, Rotmensch J, Luborsky JL (2007) Anti-tumor and anti-ovarian autoantibodies in women with ovarian cancer. Am J Reprod Immunol 57:243–249

Campbell SC, Novick AC, Bukowski RM (2007) Renal tumors. In: Wein AJ, Kavoussi LR, Novick AC, Partin AW, Peters CA (eds) Campbell-Walsh urology, vol 2, 9th edn. Saunders Elsevier, Philadelphia, pp 1567–1637

Cioffi CL, Liu XQ, Kosinski PA, Garay M, Bowen BP (2003) Differential regulation of HIF-1α prolyl-4-hydroxylase genes by hypoxia in human cardiovascular cells. Biochem Biophys Res Commun 303:947–953

Hirsilä M, Koivunen P, Günzler V, Kivirikko KI, Myllyharju J (2003) Characterization of the human prolyl 4-hydroxylases that modify the hypoxia-inducible factor. J Biol Chem 278:30772–30780

Jemal A, Siegel R, Ward E, Hao Y, Xu J, Thun MJ (2009) Cancer statistics, 2009. CA Cancer J Clin 59:225–249

Kitamura H, Honma I, Torigoe T, Hariu H, Asanuma H, Hirohashi Y, Sato E, Sato N, Tsukamoto T (2007) Expression of livin in renal cell carcinoma and detection of anti-livin autoantibody in patients. Urology 70:38–42

Larsson A, Ronquist G, Wülfing C, Eltze E, Bettendorf O, Carlsson L, Nilsson BO, Semjonow A (2006) Antiproteasome antibodies: possible serum markers for prostate cancer metastasizing liability. Urol Oncol 24:195–200

Maynard MA, Ohh M (2007) The role of hypoxia-inducible factors in cancer. Cell Mol Life Sci 64:2170–2180

Nilsson BO, Carlsson L, Larsson A, Ronquist G (2001) Autoantibodies to prostasomes as new markers for prostate cancer. Upsala J Med Sci 106:43–49

Sato E, Torigoe T, Hirohashi Y, Kitamura H, Tanaka T, Honma I, Asanuma H, Harada K, Takasu H, Masumori N, Ito N, Hasegawa T, Tsukamoto T, Sato N (2008) Identification of an immunogenic CTL epitope of HIFPH3 for immunotherapy of renal cell carcinoma. Clin Cancer Res 14:6916–6923

Shimada H, Takeda A, Arima M, Okazumi S, Matsubara H, Nabeya Y, Funami Y, Hayashi H, Gunji Y, Suzuki T, Kobayashi S, Ochiai T (2000) Serum p53 antibody is a useful tumor marker in superficial esophageal squamous cell carcinoma. Cancer 89:1677–1683

Shimada H, Nabeya Y, Okazumi S, Matsubara H, Funami Y, Shiratori T, Hayashi H, Takeda A, Ochiai T (2002) Prognostic significance of serum p53 antibody in patients with esophageal squamous cell carcinoma. Surgery 132:41–47

Sobin LH, Wittekind Ch (eds) (2002) TNM classification of malignant tumors, 6th edn. Wiley-Liss, New York

Suzuki H, Akakura K, Igarashi T, Ueda T, Ito H, Watanabe M, Nomura F, Ochiai T, Shimada H (2004) Clinical usefulness of serum antip53 antibodies for prostate cancer detection: a comparative study with prostate specific antigen parameters. J Urol 171:182–186

Takeda A, Shimada H, Nakajima K, Yoshimura S, Suzuki T, Asano T, Ochiai T, Isono K (2001a) Serum p53 antibody as a useful marker for monitoring of treatment of superficial colorectal adenocarcinoma after endoscopic resection. Int J Clin Oncol 6:45–49

Takeda A, Shimada H, Nakajima K, Imaseki H, Suzuki T, Asano T, Ochiai T, Isono K (2001b) Monitoring of p53 autoantibodies after resection of colorectal cancer: Relationship to operative curability. Eur J Surg 167:50–53

Tan EM, Zhang J (2008) Autoantibodies to tumor-associated antigens: reporters from the immune system. Immunol Rev 222:328–340

Yagihashi A, Asanuma K, Tsuji N, Torigoe T, Sato N, Hirata K, Watanabe N (2003) Detection of anti-livin antibody in gastrointestinal cancer patients. Clin Chem 49:1206–1208

Zhong L, Ge K, Zu JC, Zhao LH, Shen WK, Wang JF, Zhang XG, Gao X, Hu W, Yen Y, Kernstine KH (2008) Autoantibodies as potential biomarkers for breast cancer. Breast Cancer Res. doi:10.1186/bcr2091

Tumor-Produced Secreted Form of Binding of Immunoglobulin Protein Elicits Antigen-Specific Tumor Immunity

Yasuaki Tamura, Yoshihiko Hirohashi, Goro Kutomi, Katsuya Nakanishi, Kenjirou Kamiguchi, Toshihiko Torigoe, and Noriyuki Sato

Binding of immunoglobulin protein (BiP) is a major molecular chaperone localized in endoplasmic reticulum (ER). It has been demonstrated to interact with nascent Ig. However, contrary to other ER-resident heat shock proteins such as gp96, calreticulin, and ORP150, it is not clear whether tumor-derived BiP plays a role in inducing antitumor immunity. In this study, we show that the tumor-derived secreted form of BiP is capable of inducing antitumor CD8$^+$ T cell responses. We constructed an ER-retention signal KDEL-deleted mutant of BiP cDNA and transfected it to tumor cells, which resulted in continuous secretion of tumor-derived BiP into the extracellular milieu. We show that this secreted BiP is taken up by bone marrow-derived dendritic cells, and thereafter BiP-associated Ag peptide is cross-presented in association with MHC class I molecules, resulting in elicitation of an Ag-specific CD8$^+$ T cell response and antitumor effect. This strategy to boost antitumor immune responses shows that a tumor could be its own cellular vaccine via gene modification of the secretion of the tumor Ag–BiP complex. ***The Journal of Immunology*****, 2011, 186: 4325–4330.**

Heat shock proteins (HSPs) are molecular chaperones that control the folding of proteins and prevent their aggregation. Previous studies have demonstrated that tumor-derived HSPs initiate protective and tumor-specific CTL responses (1–5). Gp96, which is an endoplasmic reticulum (ER)-resident HSP, has been especially well studied and shown to elicit tumor-specific protective immunity (1, 6). The basis of the immunological capabilities of HSPs is thought to reflect two intrinsic properties: 1) they act as general adjuvants to the innate immune system, promoting the maturation and activation of dendritic cells (DCs), followed by the cytokine secretion required for effective T cell activation; and 2) as vehicles for associated peptides, they deliver their bound Ags to professional APCs such as DCs to yield peptide-specific T cell stimulation (7). The professional APCs such as DCs and macrophages have the ability to prime immune responses (8–10). These cells acquire Ags from donor cells such as tumor cells, then present the captured Ags via their own MHC class I molecules to CD8$^+$ T cells in a process known as cross-presentation. Recent studies demonstrated that exogenous HSP–peptide complexes were taken up by APCs through receptor-mediated endocytosis, and associated antigenic peptides were cross-presented in the context of MHC class I molecules, followed by the CD8$^+$ T cell response (11–13). Moreover, a number of cellular receptors for HSPs have been described, including CD91 (14), CD40 (15), LOX-1 (9), SR-A (16), and SREC-1 (17, 18). It is suggested that the interaction of HSP–peptide complexes with these receptors might facilitate receptor-dependent endocytosis, processing of the chaperoned peptides, and presentation of peptides in the context of MHC class I molecules. However, the precise mechanism for HSP-mediated cross-presentation in intracellular trafficking and the process for peptide trimming need to be further explored. Recently, taking advantage of the HSP–peptide complex for efficient targeting to DCs and elicitation of cross-presentation, gene therapy using secretable forms of HSPs has been developed (19, 20). Secreted extracellular HSPs from tumor cells carry antigenic peptides, and these peptides are cross-presented by DCs, leading to cytotoxic T cell responses.

Binding of immunoglobulin protein (BiP), an Ig-binding protein also known as glucose-regulated protein 78 (Grp78), is a constitutively expressed protein associated with the lumen of the ER and a member of the Hsp70 family of proteins (21, 22). In common with other members of the family, BiP has an ATP-binding domain at the N terminus and a C-terminal peptide-binding domain (23, 24). It is a broad-specificity molecular chaperone that transiently binds newly synthesized polypeptide chains and thereby assists in their correct folding and posttranslational modification. BiP is also responsible for the transfer of aberrant proteins to proteasomes for degradation, known as ER-associated degradation (25–27). It is expressed at high levels in the cell but is increased in situations that lead to accumulation of unfolded proteins in the cell and cellular stresses such as anoxia and glucose starvation. However, its role in cancer immunity remains unclear. In this study, we show that secreted BiP plays an important role in eliciting tumor-specific CTL responses through cross-presentation. By establishing tumor cells that have the ER-retention signal KDEL-deleted BiP mutant gene, we demonstrate that the secreted form of BiP chaperones tumor-derived Ags, and these Ags are cross-presented by bone marrow-derived dendritic cells (BMDCs), eliciting CD8

Department of Pathology, Sapporo Medical University School of Medicine, Sapporo 060-8556, Japan

Received for publication December 13, 2010. Accepted for publication January 4, 2011.

This work was supported in part by a grant-in-aid for scientific research and the Program for Developing the Supporting System for Upgrading Education and Research from the Ministry of Education, Culture, Sports, Science and Technology of Japan and by a Health and Labor Sciences Research grant-in aid from the Ministry of Health, Labor and Welfare of Japan.

Address correspondence and reprint requests to Yasuaki Tamura, Department of Pathology, Sapporo Medical University School of Medicine, South 1, West 17, Chuo-ku, Sapporo 060-8556, Japan. E-mail address: ytamura@sapmed.ac.jp

Abbreviations used in this article: BiP, binding of immunoglobulin protein; BMDC, bone marrow-derived dendritic cell; DC, dendritic cell; ER, endoplasmic reticulum; HSP, heat shock protein; sBiP, secreted form of BiP.

www.jimmunol.org/cgi/doi/10.4049/jimmunol.1004048

T cell responses. These findings suggest a novel strategy for cancer immunotherapy.

Materials and Methods

Mice and cells

Female C57BL/6 (H-2^b), B6C3F1 (H-2^{bxk}), and BALB/$c^{nu/nu}$ mice were obtained from Hokudo (Sapporo, Japan) and used at 4–6 wk of age. Murine thymoma cell lines EL4 (H-2^b), E.G7 (EL4 transfected with cDNA encoding OVA), CT26, LLC, and YAC-1 were obtained from American Type Culture Collection. The hybridoma cell lines B3Z and KZO were kind gifts from Dr. N. Shastri (University of California, Berkeley, CA). B3Z is a $CD8^+$ T cell hybridoma specific for the $OVA_{257–264}$ epitope (SL8) in the context of H-$2K^b$. KZO is a $CD4^+$ T cell hybridoma specific for $OVA_{246–264}$ (PL19) in the context of I-A^k. CT26 is a chemically induced murine colon carcinoma (H-2^d). LLC is a spontaneous murine lung carcinoma (H-2^b). All cell lines were cultured in RPMI 1640 medium with 10% heat-inactivated FCS. BMDCs derived from C57BL/6 and B6C3F1 mice were cultured as described previously (28). In brief, bone marrow cells from the femur and tibia were cultured in RPMI 1640 medium supplemented with 10% heat-inactivated FCS containing 20 ng/ml murine GM-CSF (R&D Systems, Minneapolis, MN). Medium was replaced on days 2 and 4, and on day 5 the cells (immature BMDCs) were harvested for use.

Construction of secreted form of BiP and generation of tumor cell line secreting BiP

Using human BiP cDNA as a template, the sense primer (5′-CCGCTCGAGATGAAGCTCTCCCTGGTGGC-3′) and the anti-sense primer (5′-CCCAAGCCTTTCTGCTGTATCCTCTTCAC-3′) were used to generate a KDEL-minus BiP cDNA. The PCR product was digested with HindIII/XhoI and ligated into the pcDNA3.1-myc/His vector. The sequence of the construct was verified by DNA sequencing. E.G7 cells and CT26 cells were transfected with constructs using Lipofectamine 2000 (Invitrogen, Carlsbad, CA). Cells were then subcloned with 1 mg/ml G418 (Invitrogen). E.G7-mock cells were transfected with the pcDNA3.1-myc/His vector and served as a control.

Peptides

The single-letter code sequences of the peptides used are as follows: H-$2K^b$-restricted SL8, SIINFEKL (positions 257–264 of the OVA protein), and I-A^k-restricted PL19, PDEVSGLEQLESIINFEKL (positions 246–264 of the OVA protein). These peptides were synthesized at Sigma Genosys (Ishikari, Japan).

Abs

The mAb anti-BiP was obtained from StressGen Biotechnologies (Victoria, VA). The mAb anti–c-myc (clone 9E10) was purified from ascites. A rabbit anti-OVA Ab was purchased from Millipore (Billerica, MA). The hybridomas, which produced mAb anti-CD8α (clone 2.43) and mAb anti-CD4 (clone GK1.5), were purchased from American Type Culture Collection.

Immunoprecipitation

To characterize the secreted form of BiP (sBiP), immunoprecipitates made with the anti–c-myc mAb and protein G beads (GE Healthcare, Tokyo, Japan) of culture media from parental E.G7, E.G7-mock, E.G7-sBiP, and CT26-sBiP cells were subjected to Western blotting using the mAb against c-myc, BiP, and the rabbit anti-OVA Ab.

Purification and quantification of the secreted BiP

The culture media (100 ml) used for 1×10^7 E.G7-sBiP and CT26-sBiP cells over 24 h were collected and centrifuged to remove cell debris. Secreted BiP was purified using a c-myc protein purification kit (MBL, Nagoya, Japan) according to the manufacturer's instructions. Briefly, the supernatant was applied onto an anti–c-myc agarose column. After extensive washing, secreted BiP was eluted off the column with PBS containing an excess amount of c-myc peptide. Otherwise, we recovered secreted BiP as a glycosylated protein from the supernatant. E.G7-sBiP cells were cultured in 3% FCS RPMI 1640 medium for 24 h, and the culture media were collected. The supernatant was applied onto a Con A–agarose column (Pharmacia). After the extensive wash, sBiP was eluted off the column with PBS containing 10 mM α-methylmannoside (Sigma). Because FCS contained glycosylated proteins such as albumin, 100 ml 3% FCS RPMI 1640 medium was applied onto a Con A–agarose column and eluted using the same procedure as described above. The resultant eluted material was used as a background protein for a micro BCA protein assay. The presence of sBiP in eluted fraction was examined by SDS-PAGE stained with Coomassie brilliant blue and Western blotting using Abs against BiP or c-myc tag. The concentration of purified secreted BiP was determined using a micro BCA protein assay reagent kit (Pierce, Rockford, IL) according to the manufacturer's instructions.

Tumor inoculation and vaccination

For the tumorigenicity assay, BALB/$c^{nu/nu}$ and C57BL/6 mice were injected intradermally with different doses of live E.G7-mock and E.G7-sBiP cells into the left flank. Tumor size was measured in two dimensions twice weekly. When mean tumor growth exceeded 20 mm in diameter, the mice were euthanized. Mice that were tumor free for more than 6 mo were rechallenged with 1×10^6 parental E.G7 cells or LLC lung carcinoma cells.

Immunotherapy against established tumors

E.G7 cells (1×10^6) were intradermally transplanted into the right back in C57BL/6 mice. When the average tumor diameter reached 3 mm, the mice were then treated twice 1 wk apart with 10^6 live E.G7-sBiP or irradiated E.G7 cells as a control, given in the left back. Tumor growth was recorded twice a week.

Depletion of T cells in vivo

Depletion of $CD4^+$ and $CD8^+$ T cell subsets was accomplished by i.p. injection of 200 μg GK1.5 and 2.43 mAb in 200 μl PBS on days −7 and −2, respectively. Depletion of $CD4^+$ T and $CD8^+$ T cells was verified by FACS analysis. Isotype-matched rat IgG was used as a control.

Induction of CTL

C57BL/6 mice were immunized with live E.G7-sBiP cells (1×10^6). One week after immunization, spleen cells were removed and stimulated with irradiated E.G7 cells. The lymphocyte cultures were tested for their ability to lyse E.G7 cells or SL8 peptide-pulsed EL4 cells.

In vitro cross-presentation assay

Day 5 BMDCs from B6C3F1 mice were cocultured for 24 h with E.G7-sBiP, wild-type E.G7, or EL4 cells. Tumor cells and DCs were separated using an 0.4-μm Transwell filter (Corning Japan, Tokyo, Japan) during coculture. Then, these DCs (1×10^5/well) were cocultured with 1×10^5 cells of OVA-derived peptide SL8-specific $CD8^+$ T cell hybridoma B3Z or PL19-specific $CD4^+$ T cell hybridoma KZO. The β-galactosidase activity was measured at the absorbance at 595 nm of the cleavage product of chlorophenol red β-pyranoside (Roche Diagnostics Japan, Tokyo, Japan).

In vivo cross-presentation

C57BL/6 mice were immunized in the footpads with 20 μg of the purified secreted form of BiP derived from E.G7-sBiP or CT26-sBiP cells. At 5 h after the immunization, popliteal nodes were removed, and DCs were isolated using CD11c MACS beads (Miltenyi Biotec, Auburn, CA). Then, B3Z cells (1×10^5) were added to the DC culture (1×10^5) in 96-well flat-bottom plates and incubated at 37°C. Twenty-four hours after incubation, absorbance at 595 nm was measured.

Statistical analysis

Each experiment was repeated at least three times. Tumor transplantation experiments were performed with five mice/group. Results are given as means ± SD. Comparisons between two groups were performed using Student t test, with a p value <0.05 considered to be statistically significant. Average tumor diameters on day 20 were statistically analyzed using the Mann–Whitney U test.

Results

Characterization of the secreted form of BiP

The C-terminal sequence KDEL of BiP serves as an ER-retention signal. Therefore, we hypothesized that deletion of this sequence should result in the secretion of BiP together with bound antigenic peptides from transfected tumor cells and might render tumors more immunogenic to allow tumor rejection by the immune system. We constructed a KDEL-deletion mutant of BiP cDNA and cloned it into the pcDNA3.1-myc/His vector. Deletion of the KDEL sequence of BiP and transfection of the cDNA into tumor cells

resulted in the continuous secretion of BiP into the culture supernatant. Using immunoprecipitates by the mAb anti–c-myc from the culture supernatant of sBiP-transfected E.G7 cells, designated E.G7-sBiP cells, Western blot analysis with an mAb specific for BiP confirmed the identity (Fig. 1*A*). Secreted BiP was purified from the culture supernatant of E.G7-sBiP cells using a c-myc–tagged protein purification kit as described in *Materials and Methods*. The level of secreted BiP in the 24-h culture supernatant was evaluated as 8 μg/ml from 10^6 E.G7-sBiP cells (Fig. 1*B*). In addition, we collected secreted BiP as a glycosylated protein using Con A–agarose column. The concentration of recovered secreted BiP was almost the same as that of the purified one using anti–c-myc agarose column.

Secreted BiP is responsible for increased tumor immunogenicity

At first, we examined whether E.G7-sBiP showed tumorigenicity equal to that of parental E.G7. E.G7-sBiP and parental E.G7 showed the same tumorigenicity when inoculated into BALB/c nude mice (Fig. 2*A*, 2*B*). To determine whether BiP secretion affected immunogenicity in vivo, C57BL/6 mice were injected with the live, secreting form of BiP-transfected or mock-transfected tumor cells, and the mean tumor diameter was monitored. As shown in Fig. 2*C* and 2*D*, mice efficiently rejected inoculation of as many as 1×10^6 E.G7-sBiP cells, whereas mice injected with 1×10^6 E.G7 cells developed tumors.

E.G7-sBiP induces an antitumor memory response

To characterize the role of T lymphocytes in the rejection of BiP-secreting tumors, we evaluated whether mice that rejected E.G7-sBiP developed a memory response, assayed as the ability to reject a secondary challenge with E.G7 or unrelated mouse lung carcinoma LLC cells. Four of five mice that rejected the primary E.G7-sBiP cells for more than 6 mo rejected a rechallenge with live E.G7 cells, but not with LLC cells (Fig. 3). Thus, the rejection was associated with the development of specific antitumor memory responses that persisted for >6 mo and were able to protect them from a subsequent tumor challenge.

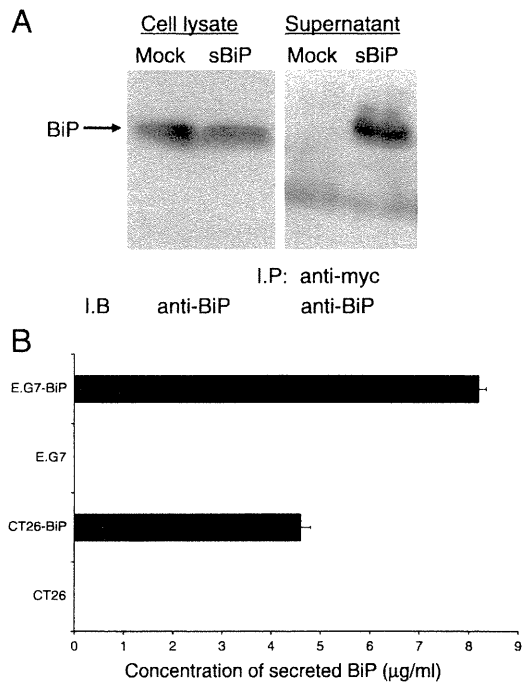

FIGURE 1. Establishment of E.G7 tumor cells expressing a secretory form of BiP. *A*, Total cell lysates and immunoprecipitates made with anti–c-myc and derived from culture media of pcDNA-mock E.G7 and pcDNA-sBiP–transfected E.G7 cells were subjected to immunoblot analysis using anti-BiP Abs. *B*, Concentration of secreted BiP from E.G7-sBiP cells. Twenty-four–hour culture media of E.G7-sBiP and CT26-sBiP cells were collected and purified using a c-myc–tagged protein purification kit. Protein concentration was measured by micro BCA assay.

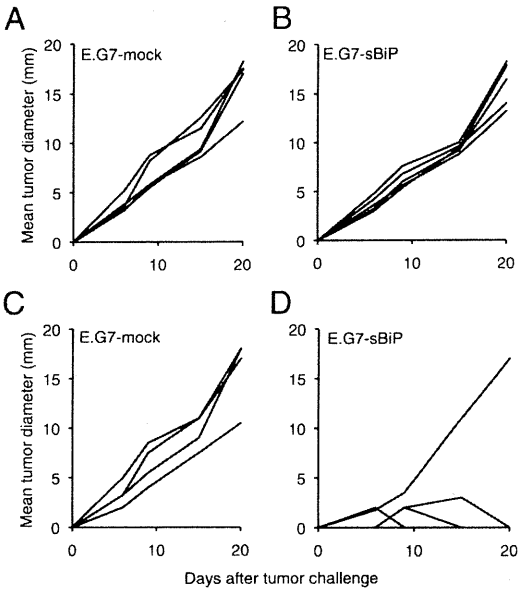

FIGURE 2. Increased immunogenicity of sBiP-transfected tumors. BALB/$c^{nu/nu}$ mice (*A*, *B*) and C57BL/6 mice (*C*, *D*) ($n = 5$) were inoculated s.c. with 5×10^6 E.G7-mock or E.G7-sBiP tumor cells. Mean tumor diameter was plotted.

Induction of tumor-specific CTL by tumor-secreted BiP

To analyze the mechanism of the increased tumor immunogenicity, we examined the ability to induce a CTL response in the mice immunized with E.G7-sBiP. Mice immunized with BiP-

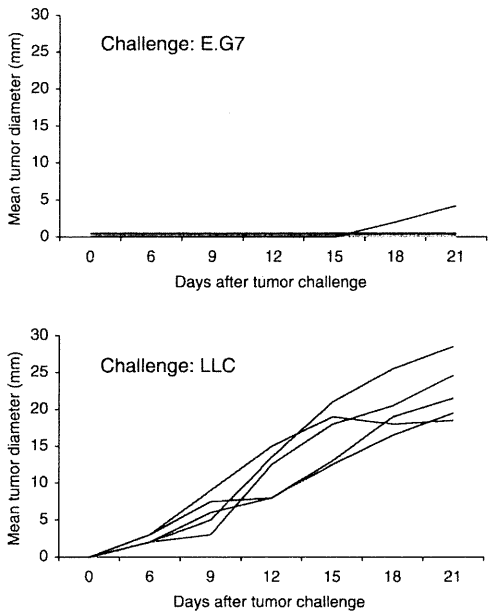

FIGURE 3. The development of tumor-specific immunity by sBiP-transfected tumors. C57BL/6 mice that rejected E.G7-sBiP cells were rechallenged with E.G7 cells ($n = 5$) or lung carcinoma LLC cells ($n = 5$). Mice were transplanted with 1×10^6 E.G7 or LLC cells, then the tumor growth rates of each group were compared using the average tumor sizes. Results shown are representative of three different experiments.

secreting tumor cells displayed a specific cytotoxic response as evaluated using OVA-positive (E.G7) and OVA-negative (EL4) cells. EL4 cells loaded with SL8 peptides restricted to H-2K^b were used to detect the response against the specific epitope SL8 of OVA. Immunization with E.G7-sBiP induced a strong CTL response against EL4 loaded with the SL8 peptide, suggesting that secreted BiP chaperoned the OVA-derived SL8 peptide restricted by H-2K^b (Fig. 4).

Involvement of immune cells in the enhanced immunogenicity

To identify the immunocompetent cells mediating the antitumor effects induced by BiP-secreting E.G7 cells, mice were depleted of the CD8$^+$ T cell or CD4$^+$ T cell subset by Ab injections as described in *Materials and Methods*. They were then injected intradermally with 1×10^6 E.G7-sBiP tumor cells. As shown in Fig. 5, in mice depleted of CD4$^+$ T cells the antitumor effect remained intact, whereas depletion of CD8$^+$ T cells completely abrogated the tumor-protective effect. These results demonstrated that the anti-E.G7–specific immunity induced by secreted BiP was dependent on CD8$^+$ T cells, not CD4$^+$ T cells.

BiP-secreting tumor shows strong therapeutic effect

To evaluate the increased immunogenicity of tumor cells secreting BiP in a therapeutic setting, E.G7 cells were first injected into the right flank and allowed to grow to ~2–3 mm in diameter, after which immunotherapy was carried out by s.c. injection of irradiated cells into the left back. Whereas treatment with irradiated E.G7 did not inhibit the tumor growth, immunotherapy with E.G7-sBiP cells markedly decreased it. Four of five mice rejected the primary E.G7 tumors (Fig. 6). Thus, secreted BiP provided antitumor activity.

Cross-presentation activity of secreted BiP–Ag complex in vitro

To determine whether secreted BiP interacted with DCs and whether chaperoned Ags were presented in the context of MHC class I and class II molecules by DCs, BMDCs were cocultured for 24 h with E.G7-sBiP, wild-type E.G7, or EL4 cells. Tumor cells and DCs were separated using an 0.4-μm Transwell filter during coculture, followed by incubation with the OVA-derived peptide SL8-specific CD8$^+$ T cell hybridoma, B3Z, or PL19-specific CD4$^+$ T cell hybridoma. Only DCs pulsed with supernatants from BiP-secreting E.G7 activated a B3Z T cell response (Fig. 7*A*). No T cell activation was detected when cells were pulsed with the supernatant from mock E.G7 or Ag-negative EL4 cells. Thus, the secreted form of BiP had the ability to chaperone immunogenic Ags and facilitate the cross-presentation of associated Ag(s). In contrast, we did not observe KZO T cell activation when the cells

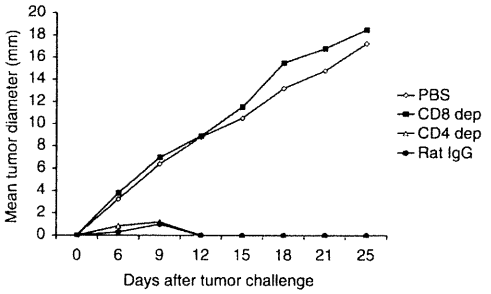

FIGURE 5. In vivo depletion assay. Mice ($n = 5$) were depleted of CD4$^+$ and CD8$^+$ T cells on days −6 and −2. They were then inoculated on day 0 with 1×10^6 live E.G7-sBiP cells. Thereafter, the tumor diameter in each mouse was recorded.

were pulsed with the supernatant from E.G7-sBiP (Fig. 7*B*). These data suggested that secreted BiP chaperoned MHC class I ligands but not class II ligands at least in the OVA Ag system. Thus, it appears that the secreted BiP chaperones antigenic peptides, and associated peptides are cross-presented by APCs such as DCs.

Immunization with tumor-derived secreted BiP elicits cross-presentation by DCs in vivo

It is very important to determine whether the cross-presentation of the secreted BiP-chaperoned Ags observed in vitro actually occurs via DCs in vivo. Therefore, we immunized mice with purified secreted BiP derived from E.G7. We confirmed that CD11c$^+$ DCs isolated from regional popliteal lymph nodes cross-presented the SL8 peptide in association with H-2K^b. Thus, the secreted BiP chaperoned the antigenic peptide, which was cross-presented by DCs in vivo (Fig. 8).

The secreted BiP purified from E.G7-sBiP cells binds OVA-derived peptides

Given that immunization with secreted BiP purified from the culture supernatant of E.G7-sBiP cells generated SL8-specific CTL responses as well as activation of B3Z, the CD8$^+$ T cell hybridoma, we speculated that secreted BiP could bind the SL8 peptide or OVA-derived precursor peptide. Therefore, we examined whether purified BiP from the culture supernatant of E.G7-sBiP cells associated with the OVA protein or its degradation products by use of immunoblotting with an anti-OVA polyclonal Ab. As shown in Fig. 9, OVA-derived degradation products could be detected in association with BiP at the molecular mass of 78 kDa, suggesting that secreted BiP chaperoned OVA-derived polypeptides, but not OVA protein, in an SDS-resistant fashion.

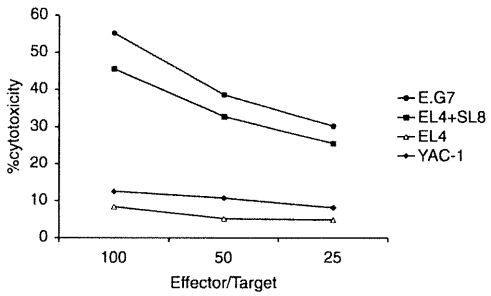

FIGURE 4. Immunization with E.G7-sBiP cells generates CTLs recognizing SL8 epitope in association with MHC class I molecules. C57BL/6 mice were immunized with live E.G7-sBiP cells (1×10^6). One week after immunization, spleen cells were removed and stimulated with irradiated E.G7 cells. The lymphocyte cultures were tested for their ability to lyse E.G7, SL8 peptide-pulsed EL4, EL4, and YAC-1 cells.

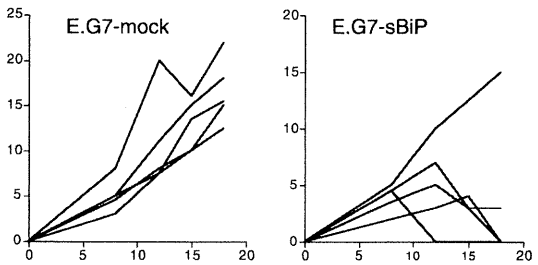

FIGURE 6. An sBiP-secreting tumor exhibits tumor-specific therapeutic activity. Mice ($n = 5$) were transplanted with parental E.G7 (1×10^5) intradermally into the right flank on day 0. The mice were then intradermally immunized in the left flank twice (on days 5 and 9) with 1×10^6 irradiated parental E.G7 or irradiated E.G7-sBiP cells.

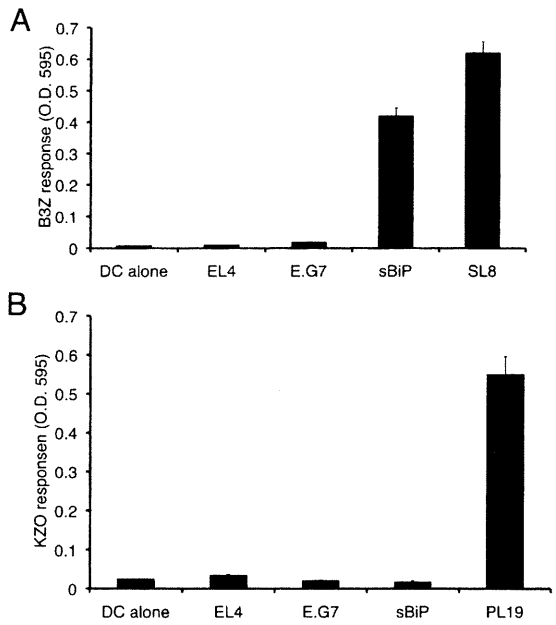

FIGURE 7. Secreted form of BiP chaperones antigenic peptide. BMDCs from B6C3F1 mice were cocultured for 24 h with E.G7-sBiP, wild-type E. G7, or EL4 cells. Tumor cells and DCs were separated using an 0.4-μm Transwell filter during coculture, followed by incubation with (*A*) B3Z or (*B*) KZO T cell hybridoma cells. SL8 and PL19 peptides served as positive controls.

Discussion

It is well demonstrated that immunization with tumor-derived HSPs such as Gp96, Hsp70, and Hsp90, and HSP complexed with an Ag peptide elicit tumor- or Ag-specific $CD8^+$ T cell responses. This protective immunity is associated with the induction of $CD8^+$ antitumor CTLs that protect mice immunized with tumor-derived HSP or in vitro-generated HSP–peptide complexes from fatal tumor loads (7). The immune response has been attributed to the ability of HSPs to form stable complexes with tumor-derived antigenic peptides, thereby facilitating the cross-presentation of MHC class I-restricted epitopes and priming of $CD8^+$ T cell responses. Moreover, a number of HSP receptors expressed on APCs have been demonstrated (29). HSP–Ag complexes have been shown to bind to these HSP receptors in a specific and saturable manner, thereby facilitating receptor-mediated endocytosis

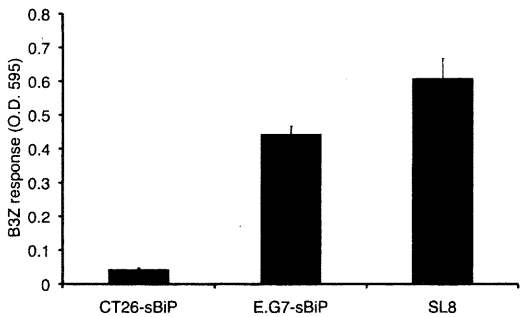

FIGURE 8. In vivo cross-presentation of antigenic peptide chaperoned by the secreted form of BiP. C57BL/6 mice were immunized in the footpads with 20 μg of the purified secreted form of BiP derived from E.G7-sBiP or CT26-sBiP cells. At 5 h after the immunization, popliteal nodes were removed, and DCs were isolated using CD11c MACS beads. Then, B3Z cells (1×10^5) were added to the DC culture (1×10^5) in 96-well flat-bottom plates and incubated at 37°C. SL8 served as a positive control. Twenty-four hours after incubation, absorbance at 595 nm was measured.

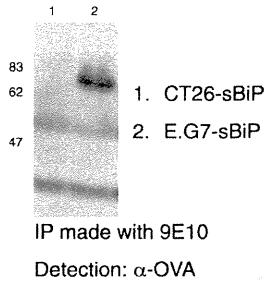

FIGURE 9. Immunoblot analysis of the secreted form of BiP using an anti-OVA polyclonal Ab. Immunoprecipitates with anti–c-myc mAbs derived from the supernatants of E.G7-sBiP and CT26-sBiP cells were dissolved by SDS-PAGE, followed by immunoblotting with the anti-OVA polyclonal Ab.

and Ag presentation. Thus, HSPs associate with antigenic peptides generated within the cytoplasm of cells and may play a role in modulating ensuing immunity toward the bound species. In addition, some HSPs stimulate innate immunity through TLRs, resulting in the enhancement of the cross-presentation of chaperoned tumor or viral peptides (30, 31).

BiP is an ER-resident chaperone for Ig and has a role in the assembly and folding of secretary proteins. It has been demonstrated that BiP interacts with its substrate peptides at the C-terminal peptide-binding domain (23, 24). However, in contrast to other ER-resident chaperones such as gp96/grp94 and ORP150/grp170, the role of BiP in tumor immunity has remained unclear. To test whether tumor-derived secreted BiP could potentially be used as an anticancer agent, the secreted form of BiP was overexpressed in E.G7 cells and tested in vivo. Deletion of the ER-retention signal KDEL of BiP resulted in continuous secretion of the BiP–peptide complex. We observed that there was a significant decrease in the tumorigenicity of E.G7 cells secreting BiP in injected mice, in addition to a significant difference in survival between mice injected with BiP-secreting cells and the control. Moreover, we confirmed that tumor-derived BiP chaperoned Ag (s), thereby leading to the induction of a tumor-specific immune response. In addition, we showed that exogenous secreted BiP was cross-presented by DCs and stimulated a peptide-specific $CD8^+$ T cell hybridoma. Furthermore, by Western blotting using an OVA-specific Ab, we showed that secreted BiP bound an OVA-derived peptide, but not OVA protein. Thus, our data indicated that secreted BiP from tumor cells chaperoned the OVA-derived peptide or its precursor peptide(s). The potential association of BiP with tumor-derived antigenic peptides may provide an insight into the immunogenicity of these associated peptides. Studies pioneered by Srivastava (7) have demonstrated that HSP-associated Ags are up to 400 times more immunogenic than Ags alone in the presentation of CD8-restricted T cell Ags to specific CTLs. It is tempting to speculate that BiP may also enhance the immunogenicity of bound tumor-derived peptides, leading to preferential uptake and presentation of Ag-specific CTLs by APCs. In this study, although we did not determine the cell surface receptor responsible for binding and uptake of BiP, a number of candidate cell surface receptors could be involved in BiP binding, including CD91 and surface Ig molecules. In addition, it is possible that, in addition to the SL8 peptide, a spectrum of antigenic peptides could be associated with the secreted BiP, behaving as a multivalent vaccine. The advantage of using a secreted form of HSP for gene transfer is that it bypasses the need to purify large quantities of HSPs. This approach allows the tumor cells to produce their own cellular vaccine. More importantly, though the secreted BiP is an exogenous protein, this serves as an efficient vehicle for Ag delivery into the MHC class I cross-presentation pathway. In

addition, whereas single peptide-based approaches have the disadvantage of a certain HLA-restricted CTL response induced by only one epitope, it is thought that a broad-spectrum antigenic repertoire is associated with BiP in the ER. Moreover, a secreted BiP-based vaccine can be used in all patients, regardless of HLA restrictions. Thus, BiP can be suitable for forming a polyvalent vaccine. Considering the clinical application of this kind of gene modification using autologous tumor cells, substantial efforts for establishing a tumor cell line, genetic modification, and validation are required. To overcome these disadvantages, use of an effective vector, for example, an adenovirus to introduce the gene for secretable BiP directly into primary tumors, may offer benefits. Thus, targeting tumor-derived chaperones to the host immune system by the method in the current study appears to be an effective means of mounting an antitumor immune response and may provide a unique therapeutic approach for cancer immunotherapy.

Acknowledgments

We thank Dr. N. Shastri for providing the B3Z and KZO T cell hybridomas.

Disclosures

The authors have no financial conflicts of interest.

References

1. Udono, H., D. L. Levey, and P. K. Srivastava. 1994. Cellular requirements for tumor-specific immunity elicited by heat shock proteins: tumor rejection antigen gp96 primes CD8+ T cells in vivo. *Proc. Natl. Acad. Sci. USA* 91: 3077–3081.
2. Udono, H., and P. K. Srivastava. 1994. Comparison of tumor-specific immunogenicities of stress-induced proteins gp96, hsp90, and hsp70. *J. Immunol.* 152: 5398–5403.
3. Sato, K., Y. Torimoto, Y. Tamura, M. Shindo, H. Shinzaki, K. Hirai, and Y. Kohgo. 2001. Immunotherapy using heat-shock protein preparations of leukemia cells after syngeneic bone marrow transplantation in mice. *Blood* 98: 1852–1857.
4. Castelli, C., A. M. Ciupitu, F. Rini, L. Rivoltini, A. Mazzocchi, R. Kiessling, and G. Parmiani. 2001. Human heat shock protein 70 peptide complexes specifically activate antimelanoma T cells. *Cancer Res.* 61: 222–227.
5. Noessner, E., R. Gastpar, V. Milani, A. Brandl, P. J. Hutzler, M. C. Kuppner, M. Roos, E. Kremmer, A. Asea, S. K. Calderwood, and R. D. Issels. 2002. Tumor-derived heat shock protein 70 peptide complexes are cross-presented by human dendritic cells. *J. Immunol.* 169: 5424–5432.
6. Tamura, Y., P. Peng, K. Liu, M. Daou, and P. K. Srivastava. 1997. Immunotherapy of tumors with autologous tumor-derived heat shock protein preparations. *Science* 278: 117–120.
7. Srivastava, P. 2002. Interaction of heat shock proteins with peptides and antigen presenting cells: chaperoning of the innate and adaptive immune responses. *Annu. Rev. Immunol.* 20: 395–425.
8. Suto, R., and P. K. Srivastava. 1995. A mechanism for the specific immunogenicity of heat shock protein-chaperoned peptides. *Science* 269: 1585–1588.
9. Delneste, Y., G. Magistrelli, J. Gauchat, J. Haeuw, J. Aubry, K. Nakamura, N. Kawakami-Honda, L. Goetsch, T. Sawamura, J. Bonnefoy, and P. Jeannin. 2002. Involvement of LOX-1 in dendritic cell-mediated antigen cross-presentation. *Immunity* 17: 353–362.
10. Ueda, G., Y. Tamura, I. Hirai, K. Kamiguchi, S. Ichimiya, T. Torigoe, H. Hiratsuka, H. Sunakawa, and N. Sato. 2004. Tumor-derived heat shock protein 70-pulsed dendritic cells elicit tumor-specific cytotoxic T lymphocytes (CTLs) and tumor immunity. *Cancer Sci.* 95: 248–253.
11. Arnold-Schild, D., D. Hanau, D. Spehner, C. Schmid, H. G. Rammensee, H. de la Salle, and H. Schild. 1999. Cutting edge: receptor-mediated endocytosis of heat shock proteins by professional antigen-presenting cells. *J. Immunol.* 162: 3757–3760.
12. Bendz, H., S. C. Ruhland, M. J. Pandya, O. Hainzl, S. Riegelsberger, C. Braüchle, M. P. Mayer, J. Buchner, R. D. Issels, and E. Noessner. 2007. Human heat shock protein 70 enhances tumor antigen presentation through complex formation and intracellular antigen delivery without innate immune signaling. *J. Biol. Chem.* 282: 31688–31702.
13. Kutomi, G., Y. Tamura, K. Okuya, T. Yamamoto, Y. Hirohashi, K. Kamiguchi, J. Oura, K. Saito, T. Torigoe, S. Ogawa, et al. 2009. Targeting to static endosome is required for efficient cross-presentation of endoplasmic reticulum-resident oxygen-regulated protein 150-peptide complexes. *J. Immunol.* 183: 5861–5869.
14. Binder, R. J., D. K. Han, and P. K. Srivastava. 2000. CD91: a receptor for heat shock protein gp96. *Nat. Immunol.* 1: 151–155.
15. Becker, T., F. U. Hartl, and F. Wieland. 2002. CD40, an extracellular receptor for binding and uptake of Hsp70-peptide complexes. *J. Cell Biol.* 158: 1277–1285.
16. Berwin, B., J. P. Hart, S. Rice, C. Gass, S. V. Pizzo, S. R. Post, and C. V. Nicchitta. 2003. Scavenger receptor-A mediates gp96/GRP94 and calreticulin internalization by antigen-presenting cells. *EMBO J.* 22: 6127–6136.
17. Gong, J., B. Zhu, A. Murshid, H. Adachi, B. Song, A. Lee, C. Liu, and S. K. Calderwood. 2009. T cell activation by heat shock protein 70 vaccine requires TLR signaling and scavenger receptor expressed by endothelial cells-1. *J. Immunol.* 183: 3092–3098.
18. Murshid, A., J. Gong, and S. K. Calderwood. 2010. Heat shock protein 90 mediates efficient antigen cross presentation through the scavenger receptor expressed by endothelial cells-I. *J. Immunol.* 185: 2903–2917.
19. Yamazaki, K., T. Nguyen, and E. R. Podack. 1999. Cutting edge: tumor secreted heat shock-fusion protein elicits CD8 cells for rejection. *J. Immunol.* 163: 5178–5182.
20. Baker-LePain, J. C., M. Sarzotti, T. A. Fields, C. Y. Li, and C. V. Nicchitta. 2002. GRP94 (gp96) and GRP94 N-terminal geldanamycin binding domain elicit tissue nonrestricted tumor suppression. *J. Exp. Med.* 196: 1447–1459.
21. Kaloff, C. R., and I. G. Haas. 1995. Coordination of immunoglobulin chain folding and immunoglobulin chain assembly is essential for the formation of functional IgG. *Immunity* 2: 629–637.
22. Lee, Y. K., J. W. Brewer, R. Hellman, and L. M. Hendershot. 1999. BiP and immunoglobulin light chain cooperate to control the folding of heavy chain and ensure the fidelity of immunoglobulin assembly. *Mol. Biol. Cell* 10: 2209–2219.
23. Wang, T. F., J. H. Chang, and C. Wang. 1993. Identification of the peptide binding domain of hsc70. 18-Kilodalton fragment located immediately after ATPase domain is sufficient for high affinity binding. *J. Biol. Chem.* 268: 26049–26051.
24. Chevalier, M., L. King, C. Wang, M. J. Gething, E. Elguindi, and S. Y. Blond. 1998. Substrate binding induces depolymerization of the C-terminal peptide binding domain of murine GRP78/BiP. *J. Biol. Chem.* 273: 26827–26835.
25. de Virgilio, M., C. Kitzmüller, E. Schwaiger, M. Klein, G. Kreibich, and N. E. Ivessa. 1999. Degradation of a short-lived glycoprotein from the lumen of the endoplasmic reticulum: the role of N-linked glycans and the unfolded protein response. *Mol. Biol. Cell* 10: 4059–4073.
26. Nishikawa, S. I., S. W. Fewell, Y. Kato, J. L. Brodsky, and T. Endo. 2001. Molecular chaperones in the yeast endoplasmic reticulum maintain the solubility of proteins for retrotranslocation and degradation. *J. Cell Biol.* 153: 1061–1070.
27. Shen, Y., L. Meunier, and L. M. Hendershot. 2002. Identification and characterization of a novel endoplasmic reticulum (ER) DnaJ homologue, which stimulates ATPase activity of BiP in vitro and is induced by ER stress. *J. Biol. Chem.* 277: 15947–15956.
28. Kurotaki, T., Y. Tamura, G. Ueda, J. Oura, G. Kutomi, Y. Hirohashi, H. Sahara, T. Torigoe, H. Hiratsuka, H. Sunakawa, et al. 2007. Efficient cross-presentation by heat shock protein 90-peptide complex-loaded dendritic cells via an endosomal pathway. *J. Immunol.* 179: 1803–1813.
29. Calderwood, S. K., S. S. Mambula, P. J. Gray, Jr., and J. R. Theriault. 2007. Extracellular heat shock proteins in cell signaling. *FEBS Lett.* 581: 3689–3694.
30. Asea, A., M. Rehli, E. Kabingu, J. A. Boch, O. Bare, P. E. Auron, M. A. Stevenson, and S. K. Calderwood. 2002. Novel signal transduction pathway utilized by extracellular HSP70: role of toll-like receptor (TLR) 2 and TLR4. *J. Biol. Chem.* 277: 15028–15034.
31. Henderson, B., S. K. Calderwood, A. R. Coates, I. Cohen, W. van Eden, T. Lehner, and A. G. Pockley. 2010. Caught with their PAMPs down? The extracellular signalling actions of molecular chaperones are not due to microbial contaminants. *Cell Stress Chaperones* 15: 123–141.

International Immunology, Vol. 23, No. 4, pp. 223–237
doi:10.1093/intimm/dxq475
Advance Access publication 18 March 2011

Extracellular heat shock protein 90 plays a role in translocating chaperoned antigen from endosome to proteasome for generating antigenic peptide to be cross-presented by dendritic cells

Jun Oura[1,2], Yasuaki Tamura[1], Kenjirou Kamiguchi[1], Goro Kutomi[1], Hiroeki Sahara[1], Toshihiko Torigoe[1], Tetsuo Himi[2] and **Noriyuki Sato[1]**

[1]Department of Pathology and [2]Department of Otolaryngology, Sapporo Medical University School of Medicine, Chuo-ku, Sapporo 060-8556, Japan

Correspondence to: Y. Tamura; E-mail: ytamura@sapmed.ac.jp

Received 5 September 2010, *accepted* 24 December 2010

Abstract

Extracellular heat shock protein can deliver associated antigens into the MHC class I presentation pathway of antigen-presenting cells, a process called cross-presentation, thus inducing antigen-specific CD8$^+$ T-cell responses; however, the precise mechanism for intracellular antigen translocation and the processing pathway has not been fully elucidated. Here we demonstrate that cross-presentation of extracellular Hsp90–ovalbumin (OVA) protein complexes to specific CD8$^+$ T cells involves both classical proteasome–transporter-associated antigen processing (TAP)-dependent and TAP-independent–endosomal pathways. Using confocal microscopy, we found that the internalized extracellular Hsp90 and OVA co-localized with cytosolic proteasomes. When anti-Hsp90 mAb was introduced to dendritic cells (DCs), we observed that the co-localization of internalized Hsp90-chaperoned OVA and proteasomes was abolished, resulting in the inhibition of TAP-dependent cross-presentation of OVA. Thus, extracellular Hsp90 may play a pivotal role for the translocation of chaperoned antigens for proteasomal degradation in the cytosol. In contrast, OVA chaperoned by Hsp90 was not presented by MHC class II molecules *in vitro* or *in vivo*, although the antigen was exogenously loaded onto DCs. Our data indicate that extracellular Hsp90 might be essential for the translocation of chaperoned antigens from the extracellular milieu into cytosol, resulting in proteasomal degradation for cross-presentation.

Keywords: antigen presentation/processing, cytotoxic T cell, tumor immunity

Introduction

Professional antigen-presenting cells (APCs), particularly dendritic cells (DCs), can take up exogenous antigens and present them on their MHC class I molecules. This process is referred to as cross-presentation and plays an important role in priming antigen-specific naive CD8$^+$ T-cell responses to tumor cells, virus-infected cells and transplants that cannot access the classical pathway for MHC class I presentation. Therefore, it is often considered in vaccination strategies aimed at improving CD8$^+$ T-cell responses. However, the exact mechanism for introduction of exogenous antigen into cross-presentation pathway remains unclear. Recent evidence indicates that exogenous antigens can be processed through at least two distinct pathways, one involving access of exogenous antigens to the classical MHC class I loading pathway [transporter-associated antigen processing (TAP) dependent] and another involving unconventional post-Golgi loading of MHC class I molecules in endocytic compartments (TAP independent) (1). One or both of these pathways can contribute to cross-presentation depending on the source of the exogenous antigens such as soluble proteins, immune complexes or peptides chaperoned by heat shock proteins (HSPs).

HSPs are molecular chaperones that control the folding of proteins and prevent their aggregation. They are capable of interacting with a broad range of peptides within the cell and the resulting HSP–peptide complexes elicit CD8$^+$ T-cell responses by cross-presentation (2). Above all, Hsp70 and gp96 have been shown to elicit efficient CTL induction by cross-presentation and anti-tumor immune responses (3–8). In contrast, it has been less elucidated whether Hsp90 is

involved in the cross-presentation. Udono and Srivastava (9) reported, for the first time, that immunization with Hsp90 purified from a tumor elicited tumor-specific CTL responses. Recently, Kunisawa and Shastri (10) reported that Hsp90 chaperoned C-terminal flanking antigenic peptides. Furthermore, Callahan *et al.* have demonstrated that endogenous Hsp90 binds N-terminal flanking precursor peptides within the cells and these peptides are cross-presented by APCs (11). We also demonstrated that extracellular Hsp90–peptide complexes generated *in vitro* were efficiently cross-presented by DCs and recognized by peptide-specific CTLs. (12). Taking these facts into consideration, it seems possible that Hsp90 is able to form highly immunogenic Hsp90–'protein antigen' complexes and to elicit antigen-specific CTL responses through cross-presentation. In this study, we therefore investigated the role of Hsp90 in the presentation of exogenous protein antigens using ovalbumin (OVA) as a surrogate antigen. We show that the Hsp90–OVA complex generated *in vitro* is efficiently and preferentially presented via the MHC class I pathway both *in vitro* and *in vivo*. Furthermore, our data suggest that extracellular Hsp90, at least in part, contributes to the translocation of chaperoned antigens from the endosomes into cytosol, resulting in proteasomal degradation. These results provide a rationale for the development of Hsp90-based vaccination strategies for cancer as well as viral immunity.

Materials and methods

Mice and cell lines

Female B6C3F1 (H-2^{bxk}) mice, C57BL/6 (H-2^{b}) mice and *TAP*$^{-/-}$ (H-2^{b}) mice were purchased from the Jackson Laboratory (Bar Harbor, ME, USA) and used at 6 weeks of age. All animal experiments were approved by the Experimental Animal Committee of Sapporo Medical University. B3Z cell is an SL8 (SIINFEKL) peptide-specific $CD8^{+}$ T-cell hybridoma that was stably transfected with the *IL-2* promoter-*lacZ* construct. When B3Z cells recognized peptide SL8 in the context of H-2Kb, activated *IL-2-lacZ* was induced and its product, β-galactosidase activity, was assayed as the cleavage of substrate chlorophenol red-β-D-galactopyranoside (CPRG) by measuring the absorbance of the cleaved product at 595 nm. As it has been shown that this β-galactosidase activity parallels the conventional IL-2 response, we compared the cross-presentation efficiency by measurement of it. The cell lines were obtained from Dr N. Shastri (University of California at Berkeley, Berkeley, CA, USA) and cultured in RPMI-1640 medium (Nissui, Tokyo, Japan) with 10% FCS (Invitrogen, Carlsbad, CA). EL4, E.G7 (EL4 transfected with cDNA encoding OVA) and YAC-1 cells were obtained from American Type Culture Collection (Manassas, VA).

Generation of bone marrow-derived DCs

Bone marrow-derived immature DCs were generated from the femurs and tibiae of female B6C3F1 mice and TAP$^{-/-}$ mice. Subsequently, 1×10^{4} bone marrow cells per well in a 24-well plate were incubated in complete RPMI-1640 with 10% FCS and 20 ng ml^{-1} granulocyte macrophage colony-stimulating factor (GM-CSF) (Endogen, Inc., Woburn, MA) for 5 days. Medium with GM-CSF was gently replaced on day 2 and day 4.

Peptides and proteins

All peptides were synthesized on a solid phase support using F-moc for transient NH_2 terminal protection and were characterized using mass spectrometry. All peptides used in this study were purified by HPLC to >99% homogeneity. The single-letter code sequences of the peptides used were as follows: H-2K^{b}-restricted SL8, SIINFEKL (positions 257–264 of the OVA protein) and I-A^{k}-restricted PL19, PDEVSGLEQLESIINFEKL (positions 246–264 of the OVA protein). Chicken OVA was purchased from Calbiochem (La Jolla, CA), and stored at 20 mg ml^{-1} in PBS at −80°C. Human Hsp90 was purchased from StressGen Biotechnologies (Victoria, BC, Canada). Quantification of endotoxin in Hsp90 and OVA was performed using the endotoxin-specific chromogenic test (ES test; Seikagaku Kogyo, Tokyo, Japan). If the endotoxin level in the Hsp90 or OVA preparation was higher than the limit of detection (<5 pg ml^{-1}), the endotoxin was depleted using Detoxi-Gel endotoxin removing gel (Pierce, Rockford, IL), after which the endotoxin was re-quantified.

Antibodies

Confocal laser microscopy was used to detect organelles with specific antibodies: an anti-Rab5 pAb (MBL, Nagoya, Japan) for early endosomes, anti-LAMP-1 pAb (Santa Cruz Biotechnology, Santa Cruz, CA) for late endosomes/lysosomes, anti-Rab11 pAb (Santa Cruz Biotechnology) for recycling endosomes, anti-KDEL mAb (StressGen Biotechnologies) for endoplasmic reticulum (ER) and anti-LMP2 pAb (Santa Cruz Biotechnology) for proteasomes. The antibodies were each conjugated with Alexa Fluor 488 (Molecular Probes, Eugene, OR) according to the manufacturer's instructions. Alexa Fluor 594 (Molecular Probes) was used for labeling with Hsp90 and OVA. A mouse anti-OVA mAb (Calbiochem), rabbit anti-OVA pAb (Sigma-Aldrich, St Louis, MO), rat anti-Hsp90 mAb (StressGen Biotechnologies), mouse anti-transferrin mAb (Sigma-Aldrich), mouse anti-Hsp72 mAb (StressGen Biotechnologies) and mouse anti-ß-Actin mAb (Sigma-Aldrich) were used in immunoblots. Rat IgG_{2a} (cloneR35-95) was purchased from BD Biosciensces (San Jose, CA).

Hsp90-protein binding

In vitro generation of the Hsp90–OVA complex was performed by the modified method described earlier (12). Hsp90 (100 μg) and OVA (200 μg) were mixed and incubated for 10 min at 45°C. The samples were then incubated for 30 min at room temperature. Samples were injected onto a HiLoad 16/60 Superdex 200 gel filtration column (GE Healthcare Japan, Tokyo, Japan) at 0.2 ml min^{-1}, and each of the fractions was analyzed by SDS–PAGE under reducing conditions; then the gels were stained for proteins using Comassie brilliant blue (Bio-Rad, Richmond, CA), followed by western blotting with the anti-Hsp90 mAb or anti-OVA mAb. To determine the binding stoichiometry of Hsp90 and OVA, protein intensities on the gel were quantified using Image-J software (NIH, Bethesda, MD). In some experiments, free Hsp90 and OVA protein were removed completely using a Microcon YM-100 (Millipore, Bedford, MA) and the purity of the Hsp90-OVA complex was examined by gel filtration

and SDS–PAGE. To confirm whether Hsp90–OVA or OVA alone aggregated during incubation at 45°C for 10 min, followed by incubation at room temperature for 30 min, the solutions were centrifuged at 16 000 × *g* for 15 min, and soluble and pellet fractions were separated, run on SDS–PAGE.

Immunoprecipitation

To confirm the generation of a complex between Hsp 90 or transferrin and OVA, the two proteins were combined at a 1:1 molar ratio and incubated for 10 min at the heat shock temperature of 45°C, followed by incubation at room temperature for 30 min. The complex was pretreated with 30 ml of protein G beads and immunoprecipitated using a mouse anti-human Hsp90 mAb, rabbit anti-OVA pAb or mouse anti-transferrin mAb. After 10% SDS–PAGE, western blot analysis was done using the rabbit anti-OVA antibody.

Antigen presentation assay

Hsp90 (100 μg), OVA (100 μg) or Hsp90 (100 μg) mixed with OVA (100 μg) for the generation of a complex were incubated for 10 min at 45°C, followed by incubation for 30 min at room temperature. This treatment did not result in the formation of a protein aggregation, which was confirmed by the method described above. In dose titration assay, DCs (1×10^5) from B6C3F1 were loaded with various doses of OVA or Hsp90–OVA complex for 2 h at 37°C in 100 μl of Opti-MEM (Invitrogen), and fixed for 1 min with 0.01% glutaraldehyde (Sigma-Aldrich). Fixation was stopped by addition of 2 M L-lysine (Sigma-Aldrich) and the cells were washed two times with RPMI-1640 medium and cultured overnight with 1×10^5 B3Z. In antigen-presentation assay, DCs (1×10^5) from B6C3F1 and $TAP^{-/-}$ mice were pulsed with Hsp90 (20 μg) alone, OVA (20 μg) alone, a simple mixture of the two, a complex of them generated *in vitro* (without removal of free Hsp90 and OVA for loading the same amount of Hsp90 or OVA in cultures), SL8 (1 μM) or PL19 (1 μM) for 2 h at 37°C and fixed and then cultured overnight with 1×10^5 B3Z or KZO. Stimulated B3Z and KZO cells were stained with CPRG (purchased from Roche, Basel, Switzerland) and red color was measured as absorbance at 595 nm.

Inhibition assay

DCs (1×10^5) from B6C3F1 mice were pre-incubated with the following inhibitors: chloroquine (Sigma-Aldrich), primaquine (ICN Biomedicals Inc., Aurora, OH), cycloheximide (Sigma-Aldrich), MG-132 (Calbiochem) and leupeptin (Calbiochem). These inhibitors were not toxic in our culture systems. Two hours after pre-incubation, the DCs were pulsed with the Hsp90 (20 μg)–OVA (20 μg) complex or SL8 (1 μM) for 2 h at 37°C in 100 μl of Opti-MEM, and then fixed, washed and cultured overnight with B3Z. Stimulated B3Z cells were stained with CPRG and red color was measured as absorbance at 595 nm.

Immunocytological localization of Hsp90–OVA complex

DCs from B6C3F1 mice were incubated at 37°C with Alexa Fluor 594-labeled OVA (20 μg), Hsp90 (20 μg) complexed with Alexa Fluor 594-labeled Hsp90 (20 μg) complexed with OVA (20 μg) for 1 h. Following incubation, cells were washed twice with ice-cold PBS, and fixed with ice-cold acetone for 1 min. Organelles were stained with an anti-Rab5 pAb for early endosomes, anti-LAMP-1 pAb for late endosomes/lysosomes, anti-Rab11 pAb for recycling endosomes, anti-KDEL mAb for ER and anti-LMP2 pAb for proteasomes, conjugated with Alexa Fluor 488 and visualized with a Bio-Rad MRC1024ES confocal scanning laser microscope system (Bio-Rad).

Endogenous Hsp90 inhibition assay

DCs (1×10^5) from B6C3F1 mice were pre-incubated with radicicol (Calbiochem). Two hours after pre-incubation with increased doses (1–5 μM) of radicicol, the DCs were pulsed with Hsp90 (20 μg)–OVA (20 μg), OVA (20 mg) or SL8 (1 μM) for 1 h at 37°C in 100 μl of Opti-MEM, and then fixed, washed and cultured overnight with B3Z. Stimulated B3Z cells were stained with CPRG and red color was measured as absorbance at 595 nm. For detecting localization of Hsp90–OVA complex, DCs were pre-incubated with radicicol at 5 μM. Two hours after pre-incubation, DCs were incubated at 37°C with Hsp90–Alexa Fluor 488-labeled–OVA complex (200 μg ml^{-1}) for 1 h and then washed and fixed. Organelles were stained with an anti-LMP2 pAb conjugated with Alexa Fluor 594 and visualized with confocal laser microscopy. To verify the effect of radicicol, following treatment of DCs with the indicated concentrations of radicicol for 2 h, the cells were further cultured for 24 h, and cell lysates then were harvested. The expression of Hsp72 was determined by western blotting with an anti-Hsp72 mAb. The β-actin level was used as a loading control.

Transduction of anti-Hsp90 antibody for blocking the Hsp90 activity within the cytosol

A rat anti-Hsp90 mAb was delivered into DCs from B6C3F1 mice using the BioPORTER protein delivery reagent (Gene Therapy Systems, San Diego, CA) according to the instructions of the manufacturer. The BioPORTER reagent forms a non-covalent complex with the antibody of interest, creating a protective vehicle for immediate delivery into cells. The hydrated mixture is added onto cells, and the BioPORTER/antibody complexes are endocytosed by the cells and then fuse with the endosome, leading to release of the BioPORTER-captured antibody into cytoplasm. One microgram of an anti-Hsp90 mAb or rat IgG_{2a} control protein was mixed with the BioPORTER protein delivery reagent and added to each dish of DCs (1×10^5). After incubation for 4 h, the medium was removed and the cells were washed with RPMI twice to remove any anti-Hsp90 mAb that did not enter the cells. The cells were incubated in the presence of the Hsp90 (20 μg)–OVA (20 μg) complex or SL8 (1 μM) for 2 h in 100 μl of Opti-MEM with pre-incubation of leupeptin (200 μM), and then fixed, washed and cultured overnight with B3Z. Stimulated B3Z cells were stained with CPRG and red color was measured as absorbance at 595 nm. At the same time, localization of internalized OVA in DCs was investigated in the presence of the anti-Hsp90 mAb by confocal laser microscopy. In addition, to examine the localization of

the transduced antibody, FITC-labeled goat IgG was added to DC culture. Organelles were then stained with an anti-Rab5 pAb for early endosomes conjugated with Alexa Fluor 594 and visualized with confocal laser microscopy.

In vivo cross-presentation assay

B6C3F1 mice were immunized in their footpads with Hsp90 (50 μg) alone or OVA (50 μg) alone or an Hsp90 (50 μg)–OVA (50 μg) complex. Draining popliteal lymph nodes were removed after 4 h, and $CD11c^+$ DCs were purified using CD11c MACS beads (Miltenyi Biotec, Auburn, CA). Purified DCs were plated at a density of 10^3 in 10% RPMI 1640 and co-cultured overnight with 1×10^5 B3Z or KZO. Stimulated B3Z and KZO cells were stained with CPRG and red color was measured as absorbance at 595 nm.

Induction of CTL

C57BL/6 mice were immunized s.c. with the Hsp90 (50 μg)–OVA (50 μg) complex, Hsp90 (50 μg) or OVA (50 μg) on days 0 and 7. Mice were sacrificed for analysis of CTL responses against the SL8 peptide. Splenocytes from immunized mice were cultured in the presence of 1 μg ml^{-1} SL8 peptide at 5×10^6 cells ml^{-1} for 5 days. On day 5, cells were harvested for standard 4-h chromium release assay.

Tumor rejection experiments

C57BL/6 mice were injected s.c. on days 0 and 7 with Hsp90 (50 μg)–OVA (50 μg), Hsp90 (50 μg) or OVA (50 μg). Seven days after the second immunization, mice were challenged i.d. with 1×10^5 E.G7 cells. Tumor size was measured in two dimensions twice a week. When mean tumor growth exceeded 20 mm in diameter, the mice were euthanized. Average tumor diameters on day 25 were statistically analyzed using the Mann–Whitney *U* test. Statistical analyses for evaluating the survival advantages on day 60 were performed using log-rank analysis. All the experiments were performed with 10 mice per group.

Statistical analysis

All experiments except for the tumor transplantation experiments were independently performed three times in triplicate. Results were given as means ± SD. Comparisons between two groups were performed using Student's *t*-test, with a P value of <0.05 considered to be statistically significant.

Results

In vitro generation of Hsp90 and OVA protein complex

To critically evaluate the capacity of Hsp90 to elicit immune responses, we carefully removed endotoxins that would activate innate immune responses. As we and others have already demonstrated, heat shock treatment accelerates the loading of antigens onto the binding sites of Hsp90 and other HSPs (12). Therefore, to generate the Hsp90–OVA complex *in vitro*, Hsp90 and OVA were mixed and incubated for 10 min at 45°C, followed by incubation for 30 min at room temperature. The resultant Hsp90–OVA complex was separated using gel filtration and each of the fractions was analyzed by SDS–PAGE. As shown in Fig. 1A, the typical pattern of elution using gel filtration for the samples presented three major peaks, and subsequent analyses by SDS–PAGE and western blotting identified the first one as the Hsp90–OVA complex, the second one as Hsp90 and the third one as OVA (Fig. 1B and C). Stoichiometric analysis using Image J software showed that the molar ratio of bound OVA to Hsp90 was ~2.0–2.2 mole OVA per mole of Hsp90. We carried out further experiments for the demonstration of the Hsp90–OVA complex. We performed co-immunoprecipitation assay using an anti-Hsp90 antibody and anti-OVA antibody. When the Hsp90–OVA complex was immunoprecipitated by the anti-Hsp90 antibody, we could detect OVA protein in the immunoprecipitates. Moreover, we performed crisscross immunoprecipitation assay using the anti-OVA antibody. We could also find Hsp90 in the immunoprecipitates. In contrast, when transferrin, as control protein, and OVA were incubated at 45°C for 10 min, followed by 30-min incubation at room temperature, we could not detect OVA in the immunoprecipitates made with an anti-transferrin antibody. These data suggested that Hsp90, but not transferrin, had the ability to generate a complex with OVA (Fig. 2A and B). To examine whether heat shock treatment caused aggregation, a mixture of Hsp90 and OVA or OVA alone was heated at 45°C for 10 min, followed by 30-min incubation at room temperature, and then centrifuged. Both the Hsp90–OVA complex and OVA were found in the soluble fractions, but not in the pellet (insoluble) fractions (Fig. 2C). These data indicated that the Hsp90–OVA complex and OVA remained soluble and did not form aggregations resulting from the heat shock treatment.

OVA is efficiently cross-presented when complexed with Hsp90 by DCs

We evaluated the cross-presentation of the *in vitro* generated Hsp90–OVA complex. To begin with, we examined the cross-presentation efficacy of exogenous OVA by DCs. As shown in Fig. 3A, the cross-presentation efficacy of OVA was considerably low even if we loaded 200 mg ml^{-1} of OVA onto DCs. In contrast, OVA was efficiently cross-presented when complexed with Hsp90 (Fig. 3B). We observed that the complex generated using 200 μg ml^{-1} Hsp90 and 200 μg ml^{-1} OVA yielded a >1000-fold increase in efficacy of the cross-presentation. Moreover, the stoichiometric analysis showed that 200 μg ml^{-1} Hsp90 could be complexed with 200 μg ml^{-1} OVA as described earlier. Additionally, we examined whether complex formation between Hsp90 and OVA was required for enhanced cross-presentation. DCs were pulsed with Hsp90 alone (200 μg ml^{-1}), OVA alone (200 μg ml^{-1}), a simple mixture of the two or a complex of them generated *in vitro* (without removal of free Hsp90 and OVA protein) for 2 h at 37°C, and then fixed, washed and cultured with B3Z T-cell hybridoma. DCs coated with peptide SL8 served as a positive control. The Hsp90–OVA complex elicited strong B3Z responses, whereas Hsp90 or OVA alone did not induce a B3Z response (Fig. 4A). Notably, when we pulsed the simple mixture of Hsp90 and OVA, we did not detect a significant B3Z response. These results showed that binding to Hsp90 was essential for cross-presentation of OVA.

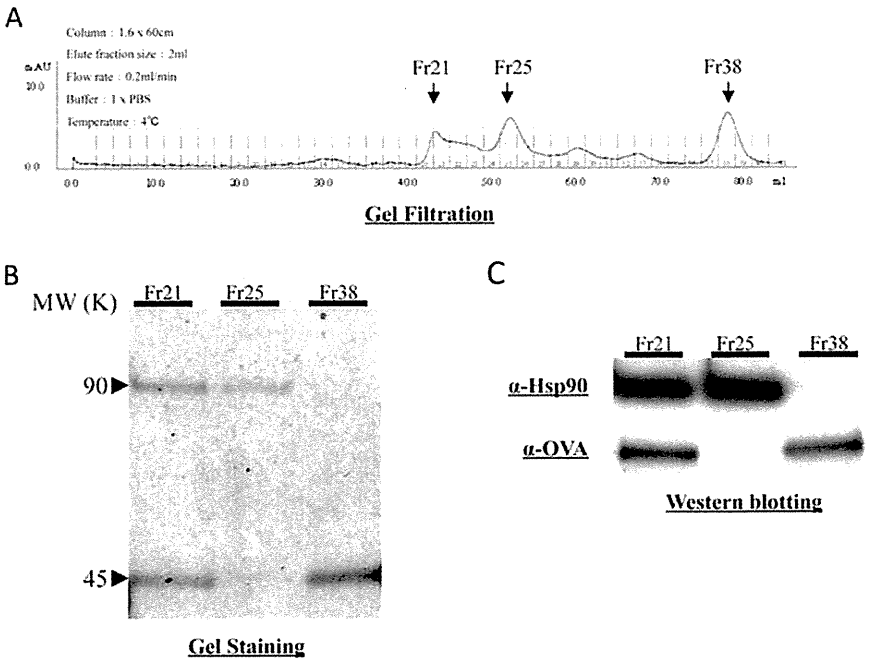

Fig. 1. Generation of Hsp90–OVA protein complex *in vitro*. (A) Hsp90 (100 μg) and OVA (200 μg) were mixed and incubated for 10 min at 45°C. The samples were then incubated for 30 min at room temperature. Samples were injected onto a HiLoad 16/60 Superdex 200 gel filtration column at 0.2 ml min^{-1}. (B and C) Each of the fractions was analyzed by SDS–PAGE under reducing conditions; then the gels were stained for proteins (B), followed by western blotting with an anti-Hsp90 mAb or anti-OVA mAb (C).

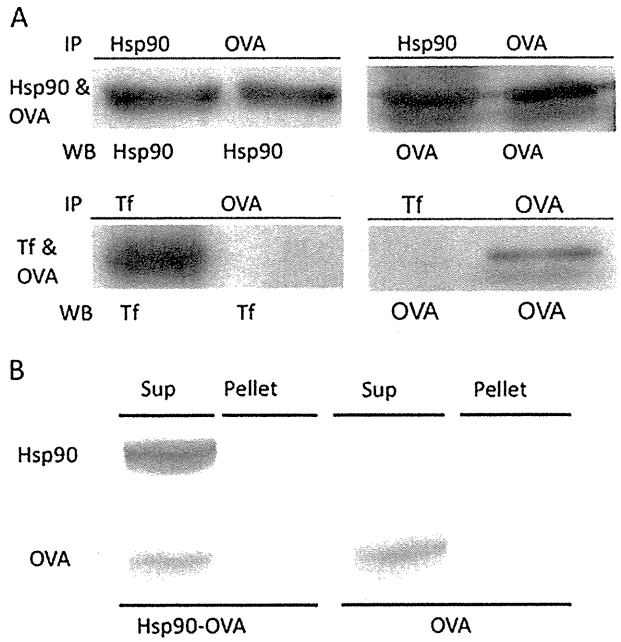

Fig. 2. Hsp90, but not transferrin, is able to bind and inhibit aggregation of client protein at heat shock temperature. (A) Direct binding of Hsp90 and OVA protein is shown by immunoprecipitation using an Hsp90 antibody and OVA antibody, followed by western blotting using the Hsp90 antibody or OVA antibody. Transferrin was used as a control protein of with a molecular weight almost the same as that of Hsp90. (B) OVA was heated to 45°C for 10 min with or without Hsp90. The total reaction mixture was centrifuged at 16 000 × *g* for 15 min to separate the supernatant and pellet. These fractions were separated and run on SDS–PAGE.

Hsp90-OVA complex is efficiently and preferentially presented through MHC class I pathway

We also tested whether the Hsp90–OVA complex was presented through the MHC class II pathway, and elicited $CD4^+$ T-cell responses. According to stoichiometric analysis, as Hsp90 binds an equal amount of OVA almost completely (i.e. no free OVA protein in the culture), DCs from B6C3F1 were pulsed with OVA alone (200 μg ml^{-1}) or Hsp90 (200 μg ml^{-1})–OVA (200 μg ml^{-1}), for 2 h at 37°C, and then fixed, washed and co-cultured with KZO $CD4^+$ T-cell hybridoma. DCs coated with PL19 peptide served as a positive control. As expected, stimulation with soluble OVA induced a strong $CD4^+$ T-cell response (Fig. 4B). In contrast, stimulation with the Hsp90–OVA complex elicited a significantly weaker $CD4^+$ T-cell response than soluble OVA. These findings suggested that the Hsp90–OVA complex was presented much more preferentially through the MHC class I pathway than the MHC class II pathway.

To examine the differences in presentation efficacy between Hsp90–OVA and free OVA, a pulse-chase experiment was performed. DCs were pulsed with OVA alone or Hsp90–OVA at 37°C, harvested at different time points between 10 min and 2 h and then fixed, washed and cultured with B3Z or KZO. B3Z responses were seen after 10–30 min of stimulation with Hsp90–OVA (Fig. 4C), although no KZO response was detected up to 1 h with OVA alone (Fig. 4D). These data demonstrated that processing and presentation of the Hsp90–OVA complex was more rapid and efficient than presentation of OVA alone.

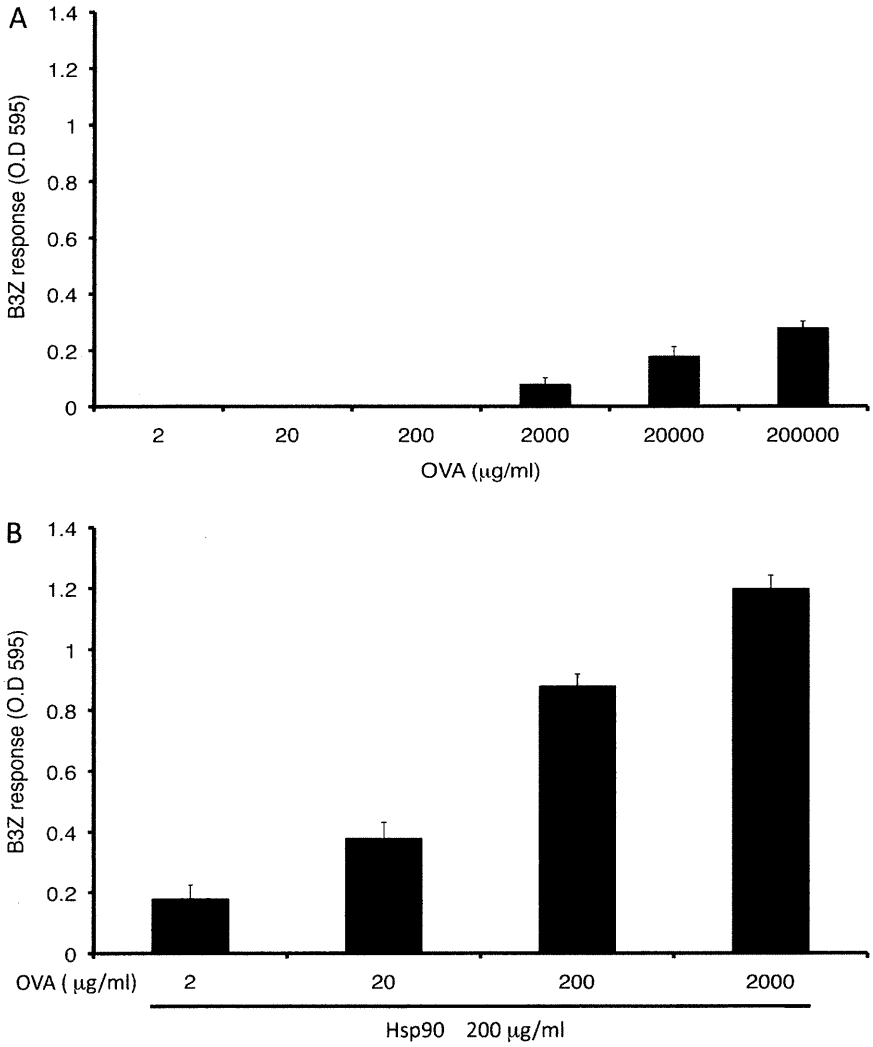

Fig. 3. OVA is efficiently cross-presented when complexed with Hsp90 by DCs. DCs (1×10^5) from B6C3F1 were loaded with various doses of OVA (A) or Hsp90–OVA complex (B) for 2 h at 37°C in 100 μl of Opti-MEM, and fixed then cultured overnight with 1×10^5 B3Z. The B3Z response was measured as β-galactosidase activity using CPRG by the absorbance at 595 nm.

Vacuolar acidification is required for cross-presentation of Hsp90–OVA complex

After internalization by DCs, Hsp90–OVA possibly enters acidic endocytic compartments. To assess if inhibition of vacuolar acidification blocked cross-presentation of the Hsp90–OVA complex, we used chloroquine. DCs were pre-incubated with increasing concentrations of chloroquine, and then pulsed with Hsp90–OVA. Chloroquine completely blocked cross-presentation at 200 μM but had no substantial effect on SL8 presentation (Fig. 4E). This showed that cross-presentation of Hsp90–OVA depended on vacuolar acidification, possibly including proteolysis by endosomal proteases. Moreover, as the Hsp90–OVA complex is expected to be taken up by receptor-dependent endocytosis, the acidic condition might be necessary to dissociate the Hsp90–OVA complex from such putative receptors.

Hsp90–OVA complex is cross-presented by both TAP-dependent and TAP-independent pathways

It is generally accepted that exogenous antigens are cross-presented by two distinct pathways in TAP-dependent and TAP-independent fashions. We examined whether cross-presentation of Hsp90–OVA depended on TAP transport. DCs from B6C3F1 or $TAP^{-/-}$ mice were pulsed with Hsp90–OVA for 2 h. Cross-presentation of the Hsp90–OVA complex by TAP-deficient DCs dropped 40–50% compared with that by B6C3F1 WT-derived DCs, whereas SL8 presentation was not affected (Fig. 5A). This indicated that Hsp90–OVA was cross-presented via both TAP-dependent and TAP-independent pathways. Antigenic peptides are considered to be loaded in a TAP-dependent manner onto newly synthesized MHC class I molecules in ER and in a TAP-independent manner onto recycling MHC class I molecules in endocytic compartments. To evaluate these processes in our system, we